PSFC/RR-09-2

Superconducting DC Power Transmission and Distribution

J.V. Minervini, L. Bromberg, P. Michael,
C. Miles, N.R. LaBounty

Engineering and Technology Division
MIT Plasma Science and Fusion Center

February 18, 2009

Superconducting DC Power Transmission and Distribution

Joseph V. Minervini, Leslie Bromberg, Philip Michael,
Christopher Miles, Nicholas R. LaBounty

Table of Contents

1. Executive Summary

The large-scale use of superconductivity and cryogenics can have substantial impact on the energy systems in the US and around the world. Increased electrification in developing countries drives a corresponding need for increased efficiency of energy use. In particular, the use of superconductivity can help minimize energy losses in the transmission and distribution (T&D) of electricity.

By using superconducting and cryogenic technology it will be possible to increase the cost effectiveness, efficiency, and capacity of the power grid and it will greatly impact our present portfolio of power sources. It may also be especially needed for large-scale implementation of renewable sources, such as wind, solar photovoltaic power, and ocean wave power. These renewable sources produce either variable frequency AC or inherently DC electric power. Often they are in remote locations, including far offshore for wind and ocean wave, and far removed from main long distance transmissions lines of the grid.

Developing new technologies that would have major impact in improving the electrical grid would require a large undertaking with massive amounts of funding. Therefore, under the MITEI Seed Fund Program we focus our efforts to explore the feasibility of a limited piece of advanced grid technology based on superconducting technology that, when fully developed and integrated into the power grid, would have the greatest potential to increase efficiency and enhance reliability and flexibility.

Noting that there is already a significant effort in the US and elsewhere to develop superconducting AC transmission lines, we focus on superconducting DC transmission and distribution. Although DC power systems were initially developed late in the 19th century and has many advantages over AC power, AC won out because it could be easily transformed to high voltages, thereby reducing the current, and thus the resistive power losses necessary to make long distance power transmission practical. With the introduction of very efficient, high power, solid-state electronics DC applications become available and attractive for much wider use in the T&D system. Going from copper to superconducting DC cables yields even more significant benefit through even greater reduction in power losses. Another important benefit is that very high powers, and very high power densities can be achieved using superconducting cables, thus allowing new avenues for integration of high power in dense urban environments. For example, superconducting power cables can increase the power carried in space-limited underground transmission corridors by a factor of 4 or higher. Because they are operated at low temperature with a nitrogen coolant/dielectric, insulation degradation and danger of voltage failure or fire is significantly reduced resulting in increased safety.

For this project we have focused on a reduced scale application of superconducting DC cables, using presently available, second generation, YBCO High Temperature Superconducting (HTS) materials. This has allowed us to explore the technology at a limited scale and determine the R&D needs which would have the highest priority impact on bringing HTS DC cables to wide scale use.

We begin the report by investigating a possible near-term, limited-scale application for HTS cables. Thus we investigate whether it is technically feasible and cost-effective to replace DC copper bus with superconducting bus. The results depend upon the power level of the data center, but more so, the costs of the superconducting tape, the cryogenic system, and the refrigerator efficiency. The model indicates that the tape and cryogenic system costs must be greatly reduced, and the refrigerator efficiency increased, before superconducting technology will have a positive economic impact for this application.

A critique of the use of superconducting transmission and distribution systems has been the cryogenic thermal loads and the associated cooling requirements. Although the use of DC eliminates the cryogenic loads due to AC fields, there are still substantial cryogenic loads. One of the main goals of this study has been to determine means of decreasing these loads.

In this report, the use of intermediate cooling stages has been evaluated as a means to decrease the cryogenic load. The impact of use results in factors of ~2 decrease in the electrical power requirement of the refrigerator, as well as less expensive refrigerators, since the temperature of operation has been increased.

The use of multiple coolants also enables very long distance transmission lines. Different cooling circuit topologies for long-distance distribution systems have been evaluated in this report. Means of eliminating substantial temperature rise of the superconductor have been found, through the use of multiple coolants or multiple coolant circuits (operating at different temperatures). Long transmission lines can be cooled in this manner, using either liquid nitrogen both circuits, or liquid nitrogen for the low temperature circuit and a different fluid for the intermediate temperature circuit.

The purpose of this report was not to develop fully optimized cryogenic systems. To do so requires substantially more work, better understanding of refrigerator performance as a function of capacity and temperatures and inclusion of the small but finite thermal conduction and convection thermal ingress, especially to the low temperature circuit. Instead the purpose of the work is to show the potential of the method for addressing key issues on implementation of HTS cables for transmission and distribution.

It has been determined that it is possible to decrease the refrigeration power by about a factor of 2 for both cryostat loads and the current leads, while allowing for low temperature rise in the low temperature circuit, facilitating long sections between recool for transmission lines.

For cooling distribution systems, it has been determined that the most attractive topology includes a separate cooling system for the current leads, operating near the boiling temperature of the coolant, high pressure nitrogen. The superconductor is cooled through a separate path, using much colder coolant, with minimum temperature rise. The solution results not only in an attractive solution for cooling the superconductor and the current leads, but also in substantial reductions of the refrigerator power requirement and minimizing the use of expensive superconductor.

The options for the additional coolant have been studied. The options include liquid nitrogen (no two-phase flow), argon, light hydrocarbons, and ammonia. The light hydrocarbons are about a factor of 2 better than liquid nitrogen. For the light hydrocarbons, the boiling temperature is lowest for methane, and increases with molecular weight. Ammonia shows a high performance, but its temperature is rather elevated. It should be stressed that the use of any of these coolants requires a more complex cryogenic system, with multiple coolants. Means of implementing multiple coolant system in the long cryostats are being actively investigated, and were not the part of this program.

A parallel effort at the Plasma Science and Fusion Center, in collaboration with Creare, a small business in Hanover, NH, has been the development of joints. [1] It is clear that compact, readily connected splices will be required, which is important for initial installation. We are also exploring options for quick disconnect joints that may not require warmup of the installed cable, in order to facilitate maintenance and repair.

The recent call for upgrading the electrical grid in the US will provide challenges and opportunities for increased utilization of DC power in the electric sector, and in particular, DC for distribution. We are coordinating with colleagues in Japan (Chubu University) and China (Tsinghua University) to further explore the potential for superconductivity applications in the electrical grid. We are also looking for collaboration in components, such as cryogenic power, joints, and improved refrigerators. In order to pursue this opportunity, we hope to be able to put together an interdisciplinary team at MIT, and to collaborate with other institutions and companies.

2. The Opportunity

There are some industrial applications characterized by consumption of high, distributed power density. One such application is data centers, or data server farms. Present electricity consumption density can be over 1 kW/m^2, with total areas of over 10,000 m^2. A second one is aluminum smelters. These and other similar applications require the local distribution of high amounts of power, consuming over 10 MW, and in some cases, as much as 100 MW. Such large specific power consumption places large demands on the electrical distribution system, which is usually copper or aluminum bus. The normal conductors are large in cross section, with lengths of a few hundred meters. The cross section is designed to allow for steady state operation with air-cooling, as well as to allow for reduced power dissipation and voltage drop along the conductor. The electrical distribution bus bars runs are typically from 200 to 500 m long, and the weight of such a system is on the order of 100-200 tons, if made from copper operating at current densities on the order of 1A/mm^2 for air-cooling. Their large size also is an issue, and may be difficult to install for the highest power systems.

In 2005, US-based data centers consumed about 1.2% of the total electric capacity in the US, at a cost of about $2.5B/year, while worldwide the values were 0.8% at a cost of

$7.2B/year. The electricity use in data centers has doubled since 2000, and it is expected to double again in the next 5 years. Substantial opportunities exist in providing energy efficient solutions. [2]

In addition to small-scale distribution, there is a large effort in the US and elsewhere to develop superconducting transmission lines.[3-6] These lines are meant for long distance transmission of power and are not optimized for short distance distribution of power. However, no work on DC superconducting transmission is being pursued in the US, although there is a small effort in Japan.[7]

It is the purpose of this work to investigate the use of much smaller superconducting distribution bus to replace the normal conducting electrical distribution bus in this high power density application, and to study the manufacturing and operation of the superconducting cables to minimize the cost of the superconductor, while allowing means for providing the many secondary feeders and joints and layout flexibility required for distributed power applications. Our investigation of the system has also provided some insight into required issues for long distance transmission, in particular the cryostat loses.

3. DC Power Distribution in Data Server Centers

Most existing data server centers today in the US are powered through AC distribution systems as shown in Fig. 3.1. Power from the grid is transformed in a substation typically from 13.8kV down to 480VAC or 240VAC. The AC power is then rectified through power converters to DC and interconnected to a battery bank UPS, and then through another set of power inverters which converts it back to AC. There is also usually a bank of diesel power generators (not shown in Fig. 3.1.) connected to the input bus side of the AC/DC converters, to provide emergency backup power in case of main grid power failure. Once converted back to AC the voltage is then transformed down to 208V and routed through a Power Distribution Unit (PDU) to a Power Supply Unit (PSU) on the server racks. The PSU provides another power conversion to 400V DC then by DC/DC conversion down to a safer, lower voltage level from 12-48V. Depending on the server, they can be fed with 12V directly or, in many cases require further voltage reduction in a Voltage Regulator (VR). [8]
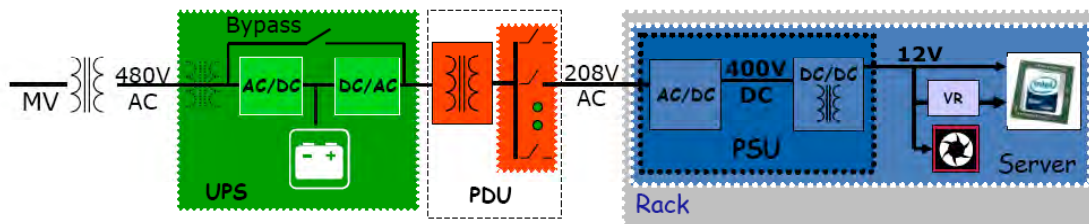

Fig. 3.1. Conventional 480 VAC power distribution system in a typical data center in the United States. [8]

These many voltage and transformations and AC/DC conversions lose a significant amount of power through device inefficiencies. For older data centers, these electrical

losses can be as high as 30-50% of the input power. Additionally, the power losses that occur within the data center building must be removed by the building HVAC system to prevent a temperature rise which would jeopardize the stable operation of the servers. That heat removal process is also inefficient. Thus for every watt lost as heat in the power distribution system, the heat rejection to the atmosphere requires an additional 1.5-2.0 watts for the HVAC system. It is clear then, that increasing the efficiency of the power distribution system can result in significant power and operating cost savings.

There is a large effort underway to increase the efficiency of AC distribution systems by operating at higher voltages, eliminating components in some instances, and by using the most highly efficient power components available. Another way of reducing power consumption in a data center is by using a DC power distribution system, as shown in Fig. 3.2, instead of AC power.
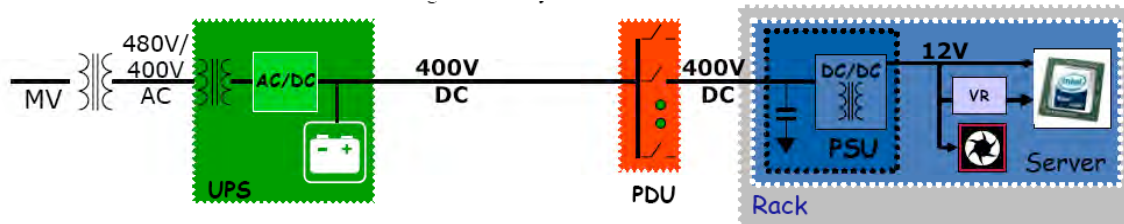

Fig. 3.2 Proposed facility level 400 VDC power distribution system.[8]

In this system, as before, AC power from the grid is transformed in a substation from 13.8kV down to 480VAC. It is then transformed to 400V followed by conversion to DC and liked to the battery UPS system. However, from this point it always remains DC (except within the DC/DC voltage converter). It is distributed as 400V DC throughout the data center and eventually to the server racks where it goes through final voltage conversion to 12V or lower for use in the servers.

It is clear then that a DC system undergoes many fewer voltage and power conversion steps then in AC system, offering the potential for significantly reduced power losses in the distribution system. Use of DC distribution in data centers was studied extensively at the Lawrence Berkeley National Laboratory (LBNL).[9] This group and a consortium of computer industry companies, built a demonstration data center project to compare the efficiencies of AC and DC distribution systems. This project demonstrated that a DC system will have an efficiency gain of 5-7% over a "best in class" AC system and a gain of 28% over an average existing data center.[10]

4. HTS Distribution System

As in resistive conductors, a superconducting wire carrying DC current has inherently lower losses than carrying an AC current. Although superconducting materials exhibit virtually zero resistance to a DC current, and AC current induces hysteretic AC and other losses in superconducting material, which can be decreased but not eliminated by

physical or geometric means. Although the AC losses in a superconductor are orders of magnitude lower than equivalent resistive losses, they still impose a heat load in the conductor system which must be removed by the cryogenic refrigerator. Since low temperature refrigerators are inherently inefficient bounded by Carnot Efficiency, the AC losses impose an operating penalty compared with a DC superconductor.

The focus of this work has been to explore if superconducting cables can be used in DC distribution systems for data centers, and further, to determine whether they offer any economic or operating advantage over conventional, resistive conductors. For this study we focused solely on replacement of the high power level carrying conductors with superconductors. That means, referring to Fig. 3.2, replacing the 400V DC cable running between the DC side of the main power converter effectively up to the PDU.
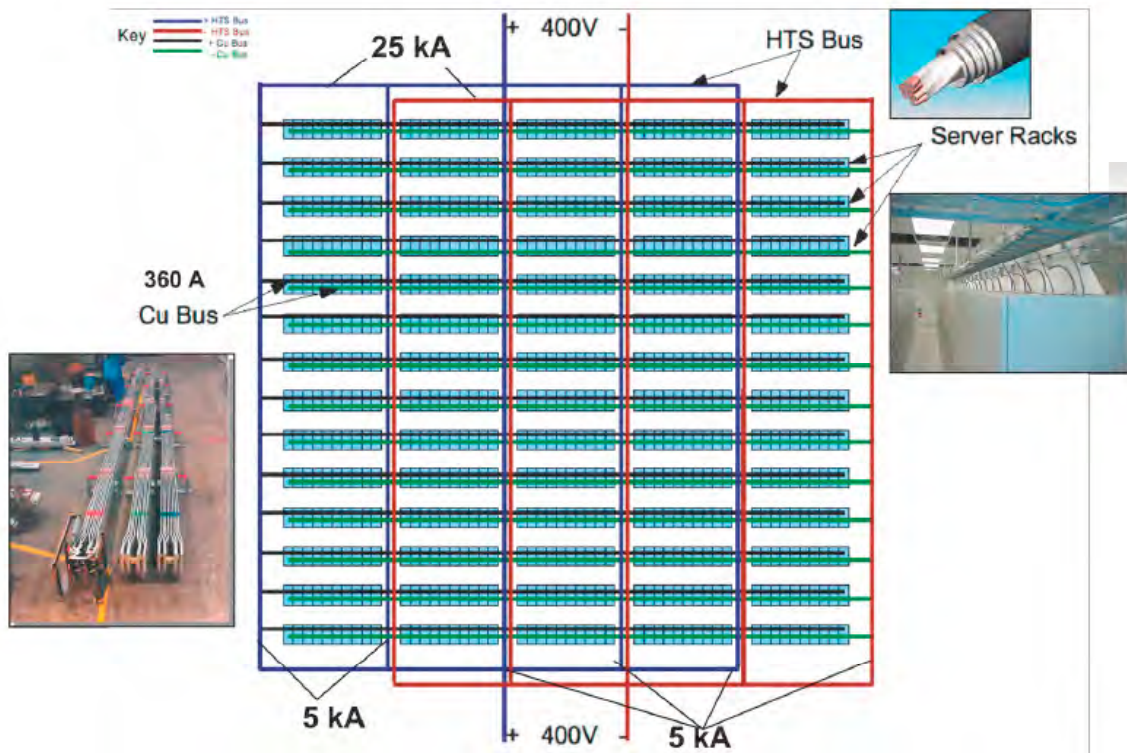
Fig. 4.1 Schematic of a data center layout using superconducting HTS cables for distribution rated at 400V by 25 kA for 10 MW of power.

For this exercise we imagined a system with the circuit schematic shown in Fig. 4.1. This layout allows us to calculate the required lengths and current levels of both superconducting and copper conductors. It also allows quantitative calculation of power losses, conductor costs, and operating costs for the electric power consumption of resistive losses in the conductors and the power consumed by the cryogenic refrigerator system.

The analysis contained in the following sections is based on the following general assumptions:

1) The data center requires 10 MW power delivered at 400 VDC.
2) Main DC power cables or bus carries 25 kA.
3) The main cable splits into 5 parallel cables, each carrying 5kA.
4) An overhead 360 A copper bus is used to distribute current to the 14 rows of server racks.
5) The system has redundant paths for the superconducting cables, effectively doubling the length of the superconductor.
6) For the case of an all copper system, rigid, rectangular copper bus is used. The bus is sized to be air-cooled, limited by either a 50 C temperature rise or a 3V voltage drop, depending on which dominates.
7) The superconductor is second generation coated conductor tape of YBCO, with properties as given in Appendix I.

The HTS cable is cooled by pressurized sub-cooled nitrogen with an inlet temperature of 65 K and a maximum outlet temperature of 75 K. These values are used to size the superconducting cable.

Using the data in Appendix I, a 25 kA superconducting cable was designed as shown in Fig. 4.2 a and b.
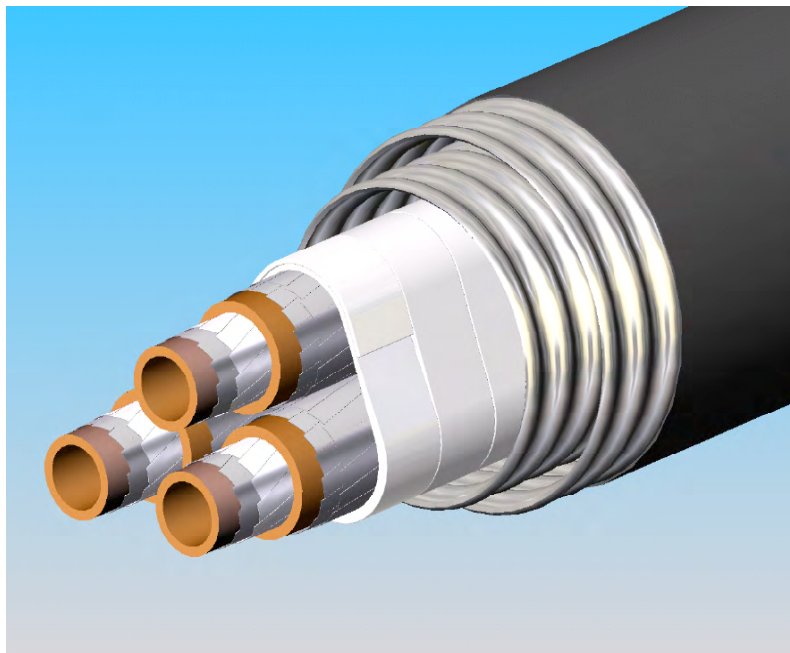
a)
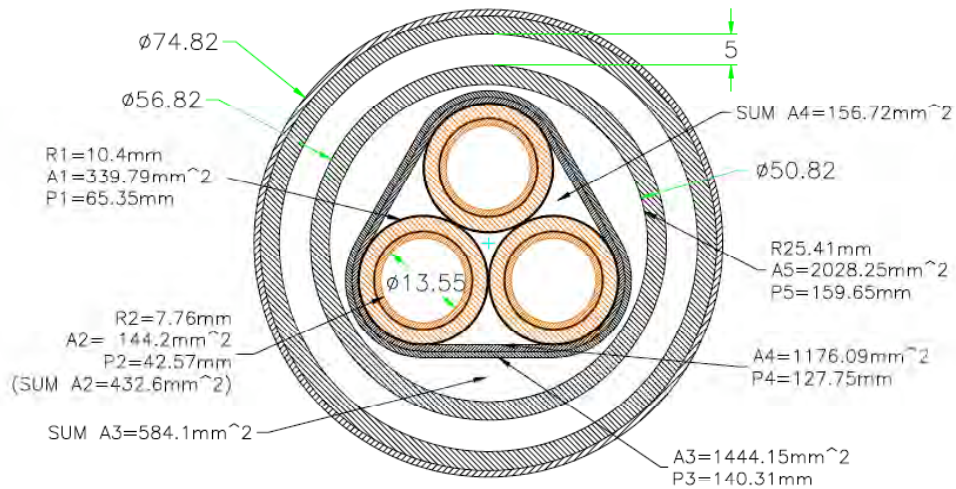
b)

Fig. 4.2 a) Sketch 25 kA HTS cable in cryostat. Each subcable contains two concentric rings of double layer tapes; b) cable and cryostat dimensions.

Based on the data center layout and conductor design there is a total of 170 m of 25 kA HTS cable and 264 m of 5 kA HTS cable.

4.1. Cost and Performance Assumptions

In 2006 the US Department of Energy commissioned a study by Navigant Consulting, Inc. entitled HTS Market Readiness Review.[11]   The purpose of the study was to investigate the HTS market and barriers to commercial entry. Tables concerning the results of this analysis are reproduced in Table 4.1 and 4.2, showing the important technology or component attritbutes, and the goals which should be achieved over different time frames in order to enter the commerical market. The values in these tables were used to perform calculations in this section, and were used to compare the attractivenes of an HTS DC distribution system with an all copper system.

Table 4.1 Performance goals for HTS conductor attributes required for market entry in different time frames.

Technology Attributes	Near-Term Goals (present – 2007)	Mid-Term Goals (2008 – 2011)	Long-Term Goals (2012 – 2016)
Critical current	250 A/cm, 77 K, sf 125 A/cm, 65 K, 2 T	500 A/cm, 77 K, sf 250 A/cm, 65 K, 2 T	1000 A/cm, 77 K, sf 500 A/cm, 65 K, 2 T
Cost/Performance Ratio	$400/kA-m, 77 K, sf $800/kA-m, 65 K, 2 T	$50/kA-m, 77 K, sf $100/kA-m, 65 K, 2 T	$10/kA-m, 77 K, sf $20/kA-m, 65 K, 2 T
Wire Length	100 m	1000 m	>1000 m
AC Losses	1 – 2 W/m	0.5 – 1.0 W/m	< 0.50 W/m

Source: NCI Analysis, Southwire, DOE.

Table 4.2 Performance goals for cryogenic and cryostat attributes required for market entry in different time frames.

	Technology Attributes	Near-Term Goals (present – 2007)	Mid-Term Goals (2008 – 2011)	Long-Term Goals (2012 – 2016)
Cryogenics	**Carnot Efficiency**	12% @ 65 K	20% @ 65 K	30% @ 65 K
	Reliability	95%	99%	> 99.9%
	Cost	$100/W @ 65K	$60/W @ 65K	$25/W @ 65K
Cable Cryostats*	**Heat Leak**	2 W/m	1 W/m	< 0.5 W/m
	Cost	$500/m	$300/m	$100/m

* Heat leak and cost goals apply to cryostats for the power cable application.
Source: NCI Analysis, Southwire, DOE.

4.2. Power Dissipation in Cryostat

Since the superconductor carries DC current there are no losses in the cable.   The cryogenic power load in DC systems is due to heat leak through the cryostat from room temperature to subcooled nitrogen temperature and through conduction/dissipation in the current leads from room temperature to the cryogenic environment. In applications for relatively compact distribution system, the cryostat heat load is negligible compared to the dissipation in the high current leads. It should be noted that this situation is reversed

for superconducting HVDC transmission lines. For that application, since there is usually only a single pair or a small number of two polarity leads at each end of a long cable, the system losses are dominated by the cryostat heat leak due to the large surface area, and current lead losses are relatively small, although they cannot be ignored for design and stability reasons.

Table 4.3 and Table 4.4 shows the power dissipation in the cryostat based on the cryostat performance given in Tables 4.1 and 4.2. The Table 4.3 is based on standard leads and the Table 4.4 is based on optimized leads as described in the following section.

Table 4.3
Power Dissipation With Standard Leads (kW)

	Power Loss HTS + Cu (2007)	Power Loss HTS + Cu (2008-2011)	Power Loss HTS + Cu (2012-2016)	Power Loss All Cu
HTS Leads	10	10	10	
HTS Cryostat	0.45	0.225	0.225	
HTS Cold Power Total	10.450	10.225	10.225	
Refrigerator Wall Power	300	177	118	
Copper Bus	16	16	16	250
Total Electrical System Power	316	193	134	250

Table 4.4
Power Dissipation With Optimized Leads (kW)

	Power Loss HTS + Cu (2007)	Power Loss HTS + Cu (2008-2011)	Power Loss HTS + Cu (2012-2016)	Power Loss All Cu
HTS Leads	5	5	5	
HTS Cryostat	0.45	0.225	0.225	
HTS Cold Power Total	5.450	5.225	5.225	
Refrigerator Wall Power	157	90	60	
Copper Bus	16	16	16	250
Total Electrical System Power	173	106	76	250

4.3. Power Dissipation in Current Leads

There are two sizes of current leads required for the superconducting cable for the datacenter; one rated at 25 kA and the other rated at 5 kA. The dissipation in these leads

dominate the losses for this system. The larger lead pairs are only required at the connections to the main cable, but there may be multiple sets of larger lead pairs for redundancy. The redundancy requirements results in additional capital costs as well as operational costs, as there will be cryogenic loads introduced even when a set of leads is not carrying current (although smaller cryogenic load).

There is a larger number of 5 kA leads because they provide the distribution along the columns serving the rows of data servers. It would not be reasonable to extend the superconducting bus to the distribution feeders above the server racks because there would too many current lead pairs which would add significantly to the system complexity and cost.

The method for computing the losses in the current leads is given in detail in Section 6. For the purpose of the analysis in this section, it is assumed that for the base case the loss in the current leads is 0.05 W/A-lead, noting that there is one lead for each polarity at each end of the cable. A second case is also considered where the optimization methods described in Section 6 are applied to reduce this loss by a factor of 2 to 0.025 W/A-lead.

Tables 4.3 and 4.4 show the lead losses in comparison with the cryostat losses (Section 4.2) as well as resistive losses in the copper bus (Section 4.5). It is clear that the current lead losses dominate.

4.4. Refrigerator Efficiency

Cryogenic refrigeration systems often have much lower efficiency relative to Carnot efficiency, and this is a strong function of both the low end operating temperature and refrigerator size as represented by the heat removal power at the low temperature side. We have used the values given the Navigant study as shown in Table 4.2. which are similar to the values in Fig. 4.1 at 65K for refrigerators in the range of 10s of kW. [12]
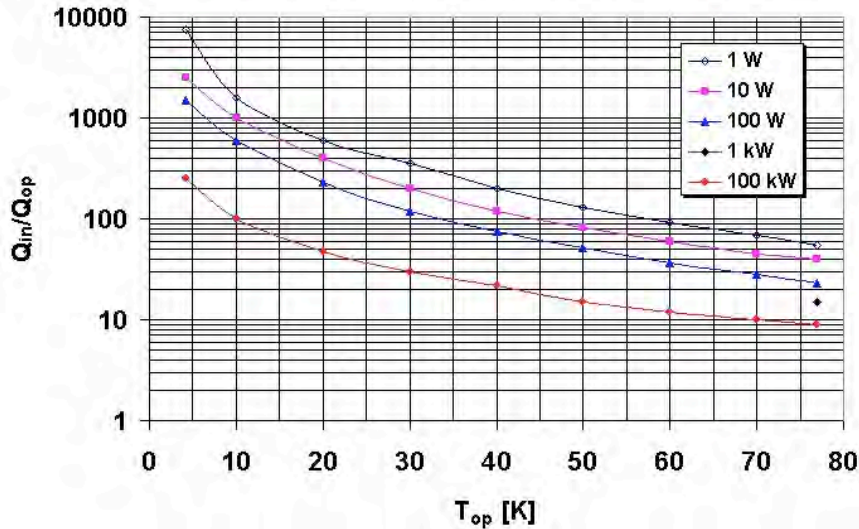
Fig. 4.3 Refrigerator performance versus T_{op} for different levels of cold end heat removal. Q_{in}/Q_{op} is the ratio of electric power required to reject the heat at room temperature relative to the ideal case where the refrigeration cycle meets ideal Carnot efficiency. [12]

4.5. Power Dissipation in Copper Bus

To carry currents at the kA level solid copper bus is often used. The bus can be sized to meet either a limit based on maximum voltage drop or temperature rise based on air-cooling. Here we size the bus to meet the criteria of either 50C maximum temperature rise or 3% voltage drop. For the system analyzed here the temperature rise was the more limiting criteria resulting in maximum voltage drop of about 2.5%. The resistive bus losses are given in Tables 4.3 and 4.4 for the case of superconductor plus copper and for the all copper system.

4.6. Capital Costs

The cost of the HTS tape, cryostat, and the refrigerator were estimated by using the values in Tables 4.1 and 4.2. The cost of copper bus was estimated using an average recent copper commodity cost of $4/kg. Installation and other costs were not considered in this study. It is expected that the copper system, being much heavier and bulky, will be more expensive that installing the superconducting system, which in principle can have a cross section of about 28 cm^2 for a 5 kA conductor. The reduced cross section and weight are especially attractive for retrofits

The copper costs at the present price are low leading to a cost advantage in comparison with the superconducting system capital costs. The capital costs are given in Table 4.5

Table 4.5
Capital Costs (k$)

	Capital Costs HTS + Cu 2007	Capital Costs HTS + Cu 2008-2011	Capital Costs HTS + Cu 2012-2016	Capital Costs All Cu
HTS Tape	2,800	560	112	
HTS Cryostat	200	130	44	
HTS Refrigerator	1,050	640	260	
HTS Total	4,050	1,330	416	
Copper Bus	11	11	11	160
Total Capital Cost	4,061	1,341	427	160

4.7. Operating Costs

For all cases the operating cost was estimated solely from the cost of electric power required at room temperature. For the case of the copper system, it is the power lost resistively in the bus. For the superconducting system, it is the power required to operate the cryogenic refrigerator which incorporates both the cryostat and current lead losses. For all cases and time periods, we assumed that power cost is $0.10/kw-hr. This is a conservative value.

It must be also noted that we have ignored the effect of lower heat dissipation in the data center building on reduction in the power required by the HVAC system to reject this heat. The refrigerator heat is rejected to the atmosphere by it's own heat exchanger outside the building, avoiding an additional load on the HVAC system. On the other hand, the resistive bus losses all go into the data center building and must be removed by the HVAC system. This is a penalty on the all copper system which could increase the operating costs by a factor of $1.2 - 1.5$ depending on the efficiency of the cooling system.

Table 4.6
Operating Cost of Power ($/hr)

	Operating Costs 2007	Operating Costs 2008-2011	Operating Costs 2012-2016
HTS (standard leads)	31.69	19.27	13.38
HTS (optimized leads)	17.26	10.62	7.61
All Copper	25.07	25.07	25.07
HTS Figure of Merit (standard leads)	Never	23 Years	2.6 Years
HTS Figure of Merit (optimized leads)	57 Years	9.2 Years	1.75 Years

4.8. Cost Analysis

Referring to Table 4.5, it is clear that capital costs of the superconducting system are always larger than an all copper system. The HTS tape cost and the cryogenic refrigerator are of comparable order, while the cryostat cost is not significant for this application.

The operating costs of the refrigerator are actually larger than the power dissipation in the all copper system in the near time frame for the standard leads, and although reduced for the optimized leads, still relatively large. If the reduction in capital costs and improvements in performance for the intermediate and longer range time frames come to fruition as given by the Navigant study, then the comparison with an all copper system is improved.

A simple figure of merit is computed by dividing the capital costs by the operating costs for all the cases that were considered. This figure of merit has a value of years and is related to a payback period, but does not take into the cost of money and depreciation. It is clear that, in the present time frame, a superconducting distribution system for a data center is not cost effective at all. The situation improves in the intermediate time frame, but only if an optimized current lead can be developed. The best situation occurs in the longer time frame where the superconducting system figure of merit is on the order of 2-3 years, and then continues to return economic value for the life of the system.

Thus it is clear that, from an economic standpoint, significant reductions in HTS tape and refrigerator costs must be achieved, as well as large improvements in conductor, refrigerator, and current lead performance in order to use an HTS distribution system for this application. Clearly the higher load imposed by the all copper system on the HVAC system power, as well as the higher installation costs, needs to be included in a further analysis. This will move the advantage toward the superconducting system, resulting in shorter payback period for all time frames.

This analysis was performed for a specific point design of a 10 MW distribution system in a data center. Further analysis over a higher range of power may show advantages for a superconducting system in the nearer time frame. Also, introduction of superconductivity to a DC distribution system may offer other advantages. For example, the power density of a superconducting cable is on the order of 3-4 times higher than a copper bus. Thus a superconducting system will occupy much less space inside the building. Copper bus is rigid, heavy, and difficult to install, especially as power levels in data centers increase. A superconducting cable in a flexible cryostat is quite light and should offer installation advantages. A major drawback though is that quick connect cable/cryostat joints should be developed as well as improved methods for installing the current leads and lead breakouts.

The following sections focus on optimization of the cryostat and current lead losses, for both transmission and distribution systems. Optimization of these components will

improve the opportunities for deployment of HTS superconducting systems in the grid and commercial power sector.

5. Cryostat Optimization Through Multiple Stage Thermal Shields

5.1. Introduction

For transmission applications, the cryostat losses are dominated by distributed thermal loads, as the losses in the current terminations are small compared with distributed losses along the superconducting transmission line. In these applications the lines operate at relatively high voltages and relatively low currents, compared with power distribution cables. This is done to minimize AC current losses in the cable.[3]

In the application of HTS cables for long distance DC transmission, the AC loses in the conductor are eliminated. Under these circumstances, thermal radiation over the long length of cryostat represents a substantial and dominant heat input to the cryogenic environment.

Multilayer insulation (MLI) is commonly used to reduce the radiant thermal load to the cryogenic environment. MLI consists of multiple sheets of metalized layers separated by non-conducting spacers. The layers are usually made from a plastic (mylar or kapton), metalized with aluminum on either one or two sides. The concept was initially proposed by Sir James Dewar.[13]

Means of minimization of the thermal loses in cryogenic environment have been discussed in the past, mainly for applications to cryogenic environments aboard spacecraft. For that application, an additional major requirement is the minimization of the weight of the system.

In this section, we investigate the minimization of the refrigeration power for cryostats to be used for transmission and distribution cables using high temperature superconductors. The cryostat MLI shields are located between the room temperature shell (298 K) and the cold cable shell (66 K), but the radiated thermal load is intercepted at intermediate temperatures with separately cooled heat stations. The use of multiple intermediate temperature stations is analyzed for both thermal radiation and thermal conduction cryogenic loads.

5.2. Model

The analysis of thermal shield using Multi-Layer Insulation (MLI) is in principle very simple. The ideal system consists of thermally insulated layers, each with a constant emissivity, operated in vacuum.

In this analysis, we simplify the calculations using an ideal model, ignoring certain factors such as perforations in MLI used for supports, lead connections, and conduction across different layers in contact. To meet this condition for conduction, the sheets must have a small thermal conductance in the radial direction. This requires precaution during design, manufacturing, and operation of the system in order to adequately meet these conditions and, thus, to approach the results later mentioned in this section.

The radiated power to a plane surface with a temperature T_c facing a plane surface at temperature T_h is given by

$$W = \sigma\, (A_h \varepsilon_h T_h{}^4 - A_c \varepsilon_c T_c{}^4)$$

where A_h and A_c are the illuminated areas, ε_h and ε_c are the surface emissivities and σ is the Stephan Boltzman constant.

The emissivity of the surface depends on the nature of the material, the history of the material (strain-hardened or soft, contamination), and thickness. In order to obtain maximum reflectivity, the thickness of the coatings needs to be on the order of a few hundred nanometers. Gold and aluminum are preferred materials.

Another complicating fact is that the emissivity is a function of temperature. Constant emissivity will be investigated first. This implication of varying emissivity will be presented in a later section.

In the presence of N shields between two surfaces (assumed parallel planes in this calculation), the thermal radiation can be shown to be[14]

$$W = A\, \varepsilon\, \sigma\, (T_h{}^4 - T_c{}^4) / (N + 1)$$

Under steady state conditions, as there are no convection thermal paths, the power radiated across each vacuum gap between thermal layers is a constant. The heat transferred due to conduction through structural supports will be discussed in a later section.

The proposed method to minimize the power requirement is to place one or multiple temperature stations throughout the thermal insulation, in order to intercept the power from the region of higher temperature. To maintain the temperature of the intermediate station at the given temperature, it is necessary to remove heat. This is done with a refrigerator that operates at the intermediate temperature.

In order to determine the electrical power requirement for the overall refrigerator system, an assumption needs to be made with respect to the efficiency of the refrigerators. It is assumed that the refrigerator efficiency is a constant fraction of the Carnot efficiency between 323 K (for air-cooled compressors) and the cold end operating temperature of the refrigerator. A relatively conservative multiple of 5 (i.e., 20% of Carnot efficiency) is used for all refrigerators, independent of temperature and capacity. This is a simplifying

assumption as it is known that the fraction of Carnot efficiency for a given refrigerator is a weak function of the refrigerator capacity.[15]

The electric power requirement for an individual refrigerator P_E is thus,

$$P_E = 5 \ Q/\eta_{Carnot}$$

where $\eta_{Carnot} = T_L/(T_H - T_L)$ is the Carnot efficiency of the refrigerator operating between upper temperature T_H and lower temperature T_L. The total electrical power is the sum of the electrical power of the individual refrigerators.

The minimization function is the electrical power. Alternatively, the minimization function could be the capital cost of the overall refrigeration system, or the cost of ownership (capital and operating costs).
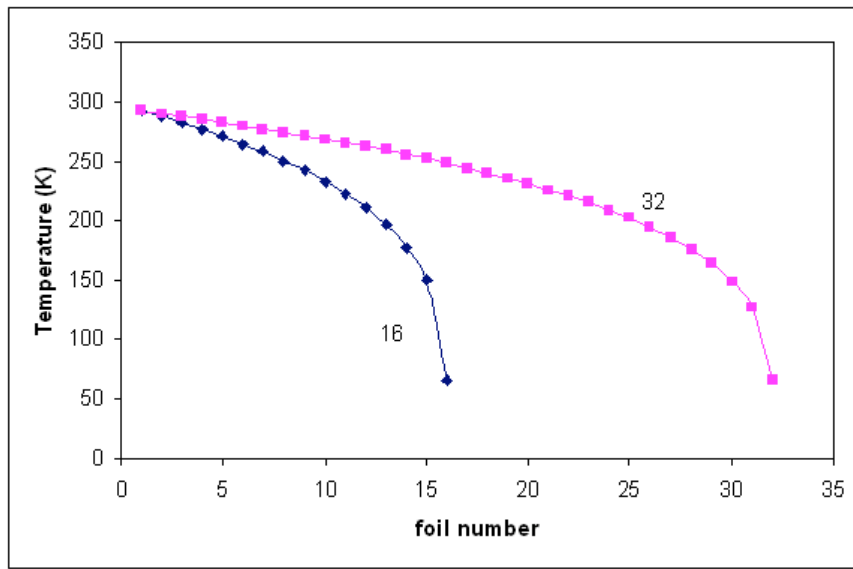

Fig. 5.1. *Temperature of the thermal shields for the case of 16 and 32 shields, for e = 0.07*

5.3. Thermal Radiation Minimization for Constant Emissivity

The results for the case of shields with emissivity ε of 0.07 and constant with temperature are presented in this section. Three cases are considered; without intermediate temperature stations, and with 2 or 3 temperature stations.

Results for the case of 16 and 32 shields without intermediate temperature stations are shown in Fig. 5.1. The temperature profile of the thermal shields is relatively flat at the higher temperature region, with most of the temperature gradient at the lower temperatures.

It is assumed that the upper temperature of the cryostat is 293 K, and the lower temperature is 66 K. Assuming that the inner diameter of the cryostat pipe is 12.7 cm, the thermal load for the case of 32 thermal layers is 0.37 W/m, with an associated electrical power of the refrigerator of 7.32 W/m. It is assumed that the upper temperature of the refrigerator is 323 K (assuming air as the thermal sink).
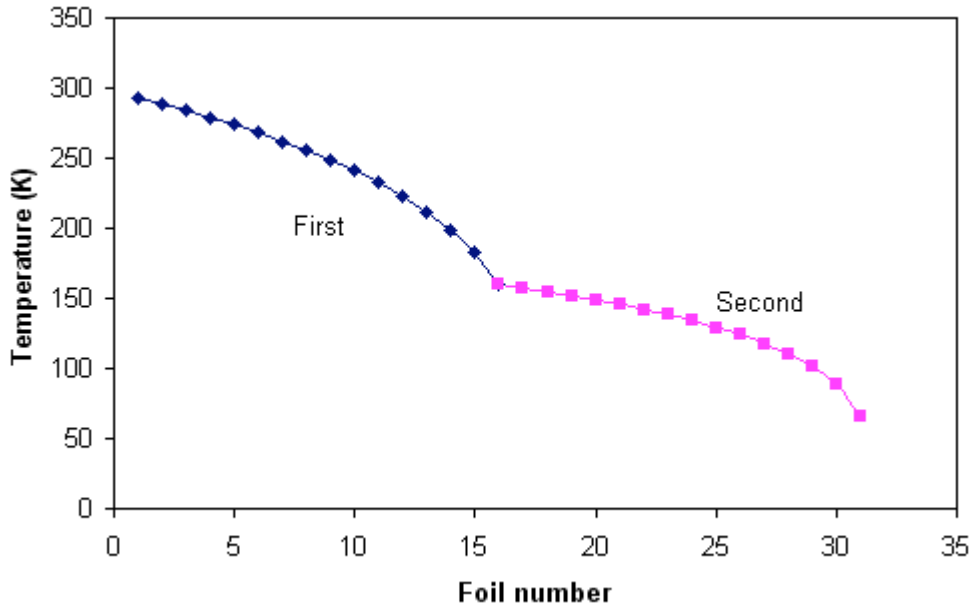

Fig. 5.2.   Temperature of the thermal layers for the case of one temperature station, at an intermediate temperature of 160 K.

The case with one temperature station of 160 K located at layer 16 is shown in Fig. 5.2. As in the previous case, there is a larger temperature gradient at the lower temperatures, for both the upper stage and lower stage.

The thermal load to the 66K refrigerator decreased to less than 0.07 W/m. The associated electrical refrigerator power decreased from 7.3 W/m to 1.2 W/m, or about 80% reduction. Note that it is necessary to cool the intermediate temperature station with a thermal load that is about the same as that of the case of 16 layers without temperature stations, about 0.7 W/m. However, the temperature of operation of the refrigerator is higher, thus decreasing the total electrical power required.

Fig. 5.3 shows the electrical power requirement for the single stage (7.3 W/m) for 32 layers. The electrical power requirement for the two-stage system is shown separately as a function of the temperature for each temperature station, as well as the total electrical power. The total electrical power minimizes at an intermediate temperature around 180 K, but it is relatively flat. It may be more useful to decrease the size of the lower temperature refrigerator further, at the expense of a slightly larger intermediate temperature refrigerator.
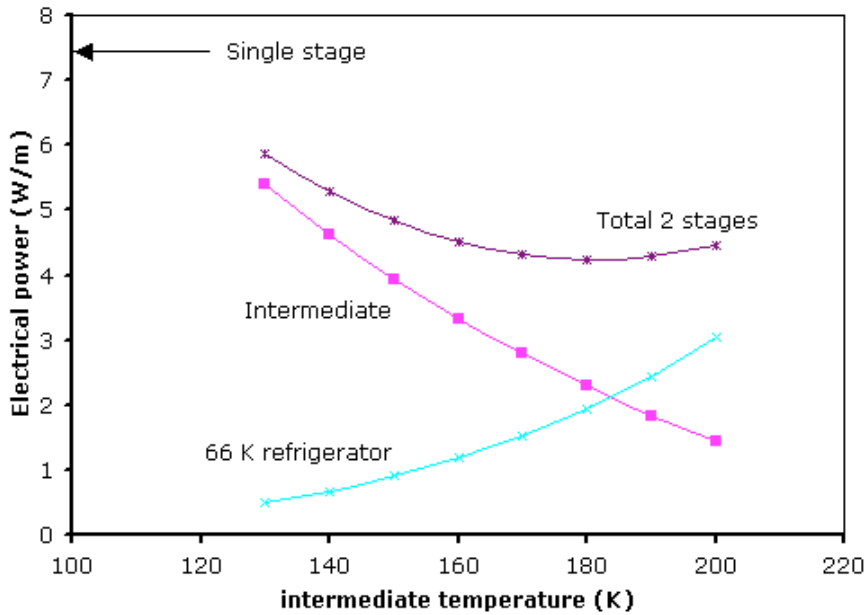
Fig. 5.3. Electrical power required to remove radiation loads for the case of no intermediate temperature station (single stage with 32 layers) and for two stages, as a function of the temperature of the intermediate stage.

As compared with the single stage electrical requirement of about 7.3 W/m, the two-stage system has a room temperature power requirement of about 4.5 W/m, or ~38% decrease.

By subdividing the warm-cold gap into two stages, the load to the 66 K refrigerator was greatly reduced although at the same time, placing a significant load on the 160 K refrigerator. The hypothesis was that this displacement of the thermal load would be beneficial overall. The main driving idea to this hypothesis was that the intermediate refrigerator is capable of handling a larger load since the operating temperature is greater than that of the lower refrigerator. This method of displacing the load to the 160 K refrigerator would hopefully greatly decrease the overall electrical power requirement. The power radiated by the room temperature surface to the colder temperatures is $\sim T^4/N$. By reducing the number of layers between the room temperature and the intermediate stage by a factor of 2 (16 layers instead of 32 layers), the radiated power intercepted by the intermediate temperature approximately doubled. The higher efficiency of the higher temperature refrigerator more than makes up for the increased radiation, reducing the electrical power, but with a net reduction of only 38% compared to the single stage case.

The case with three stages is described next. In this case, there are two arbitrarily chosen temperatures of the intermediate stages. Fig. 5.4 shows the temperature of the different layers. It is assumed that there are 16 layers per stage. Note that the overall temperature profile looks much more linear than the one shown in Fig. 1.
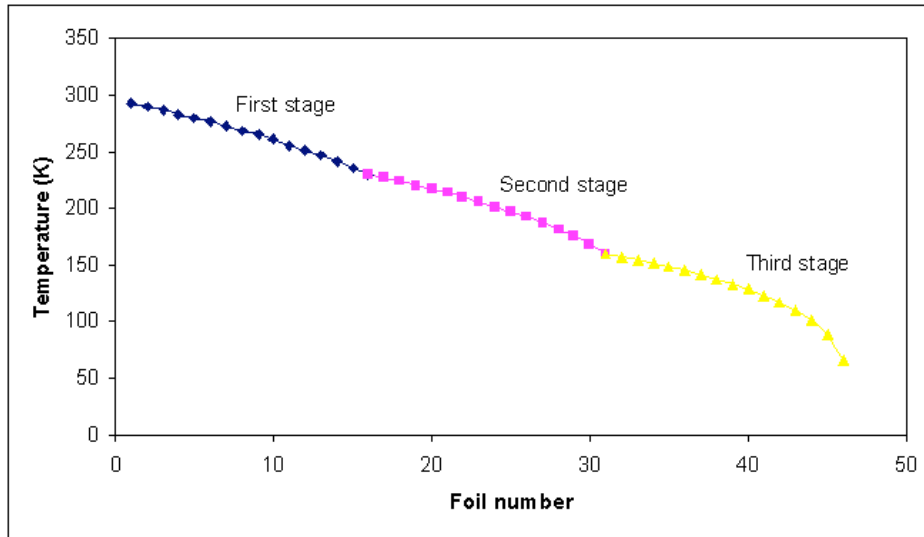
Fig. 5.4. *Temperature across the thermal shield for the case of 3 stages, 16 layers per stage.*
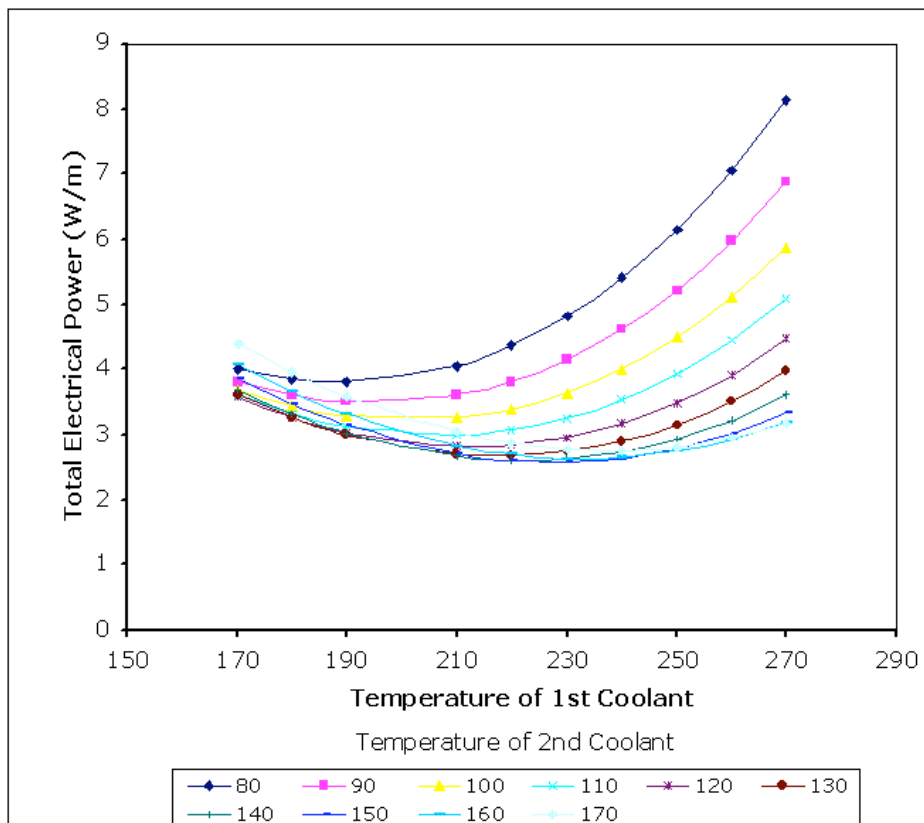
Fig. 5.5. *Electrical refrigeration power for the case of 3 stages, as a function of the intermediate stages temperatures.*

There is a broad minimum for a temperature of the upper stage of about 230 K and the second stage temperature about 150 K. The electrical power is now reduced to less than 3 W/m. Because the optimum occurs with a temperature of the second stage similar to that of the 2-stage optimization (around 140-150 K), the thermal power to the 66 K

environment is similar in both cases. The electrical power reduction is due to a decrease of the power required by the higher temperature stage.

5.4. Thermal Radiation Minimization for Temperature Dependent Emissivity

In this section, the variation of emissivity of the shells due to the variation of temperature is included in the analysis. In this analysis, emissivity is modeled as a decreasing linear function of temperature, which ranges from .07 at 293 K to .058 at 66 K. [14] The calculated temperature profiles for the single stage and two-stage models are illustrated in Figs. 5.6 and 5.7, respectively. From these two plots, it is clear that the variation of emissivity across the shells has a small affect on both models compared to the case with constant emissivity.
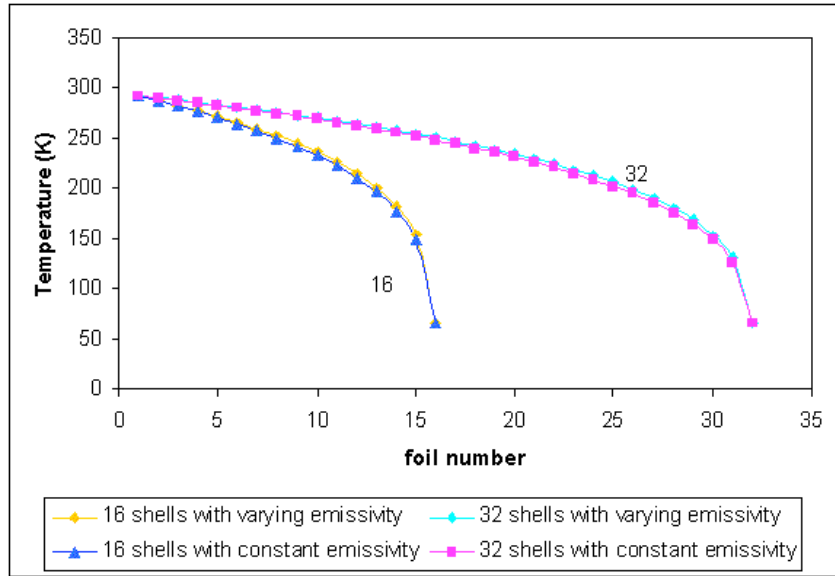

Fig. 5.6. Single stage temperature profiles for temperature dependent emissivity and constant emissivity.
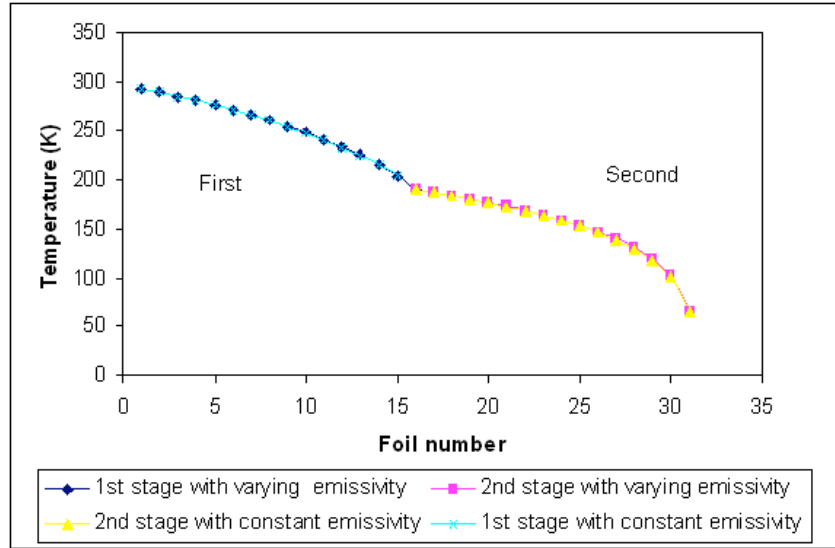
Fig. 5.7. Two-stage temperature profile across shells for temperature dependent emissivity and constant emissivity.

These results show that the analysis in the previous section with constant emissivity over this temperature range is sufficient for understanding these systems.

5.5. Thermal Conduction Through Structural Supports

Another thermal path between the coolant to the surrounding atmosphere is conduction through the structural supports/spacers. The cryogenic load is dependent on the geometry and choice of material of these supports. Two models that differ in both aspects were analyzed.

5.5.1. Models

The first model uses stainless steel tubing, bent into a triangular-like geometry (see Fig. 5.8). The tube diameter is 2 mm and the wall thickness is 0.25 mm. The inner pipe sits within the triangular support forcing the sides of the triangle to bend. The inner pipe is not welded or attached to the triangular frame to reduce thermal conduction through these contact points. However for this analysis, we use the conservative assumption of perfect thermal contact to give an upper bound to the coolant load.

The second model uses a 1 mm thick triangular sheet of either G-10 or Teflon with a circular cutout for the inner pipe (shown in Fig. 5.9). The vertices of the triangular sheet are assumed to be in intimate contact with the outer pipe.
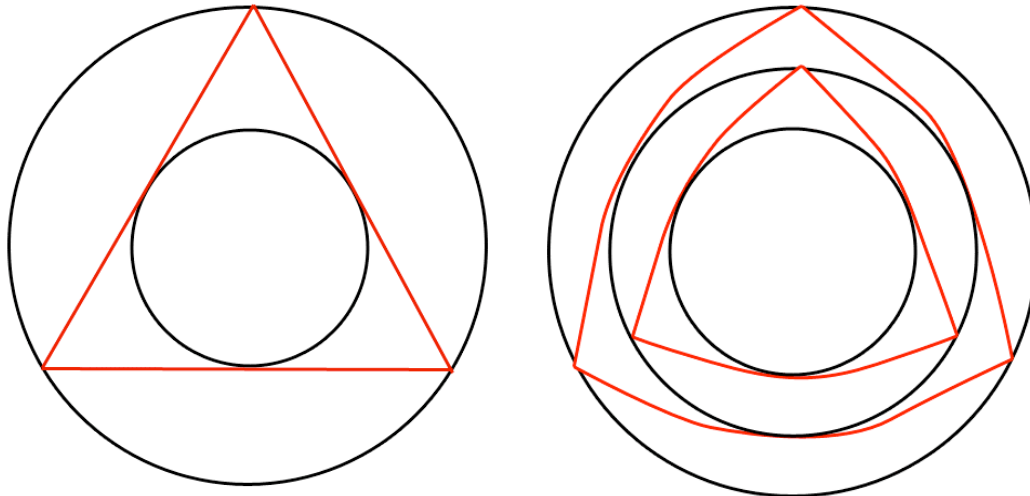
(a)   (b)

Fig. 5.8. Stainless steel supports for (a) single stage and (b) two stage cooling.
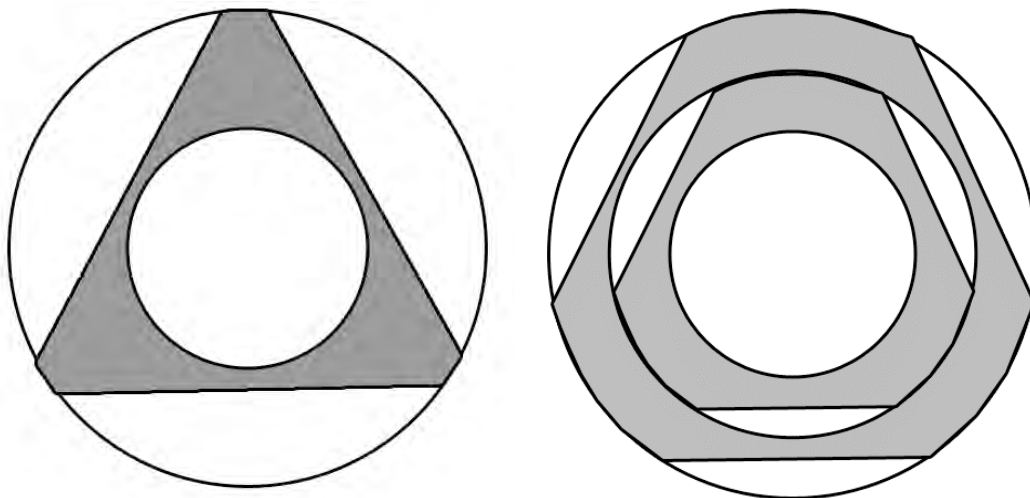
(a)   (b)

Fig. 5.9. G-10 or Teflon supports for (a) single stage and (b) two stage cooling.

5.5.2. Analysis

For each model, we compared one stage and two-stage cooling as we described above for radiation. The two-stage cooling design has two supports. One sits between the outer shell and the intermediate shell. The other support sits between the intermediate shell and the inner shell. The temperatures of the outer shell, intermediate shell, and inner shell were 273K, 150K, and 66K, respectively. For both types of supports, the radii of the outer shell, intermediate shell, and inner shell were 80mm, 60mm, and 40mm respectively. The supports were spaced 1 meter apart along the cryostat.

The radiation from the surface of the supports is negligible compared with the conduction load. The rate of heat transfer from one shell to the next is calculated by using the following heat conduction equation along one dimension,

$$Q = -A\,k\,(dT/dx)$$

where Q is the amount of heat flowing through a material per unit time, A is the cross sectional area, k is the thermal conductivity which is function of temperature. The term dT/dx is the spatial temperature gradient. While keeping Q constant (system is in steady state) and A constant, the following equation is obtained. [14]

$$Q = (A/\Delta x)\int k(T)dT$$

Here Δx is the distance between two thermal contact points. The limits of integration are the temperatures of the two contact points. This one dimensional heat equation works well for analyzing the configuration shown in Fig. 9 for the stainless steel support rods. However, we had to make an approximation for the G-10/Teflon supports by modeling the triangular plate as three 1mm thin rectangular sheets that connect the inner pipe to the outer pipe. Each rectangular sheet had a width equal to the radius of the inner pipe and a length equal to the difference between the two radii. Fig. 10 shows the temperature distribution and heat flux vector field across the support for Teflon. The temperature distribution for G-10 is almost identical.
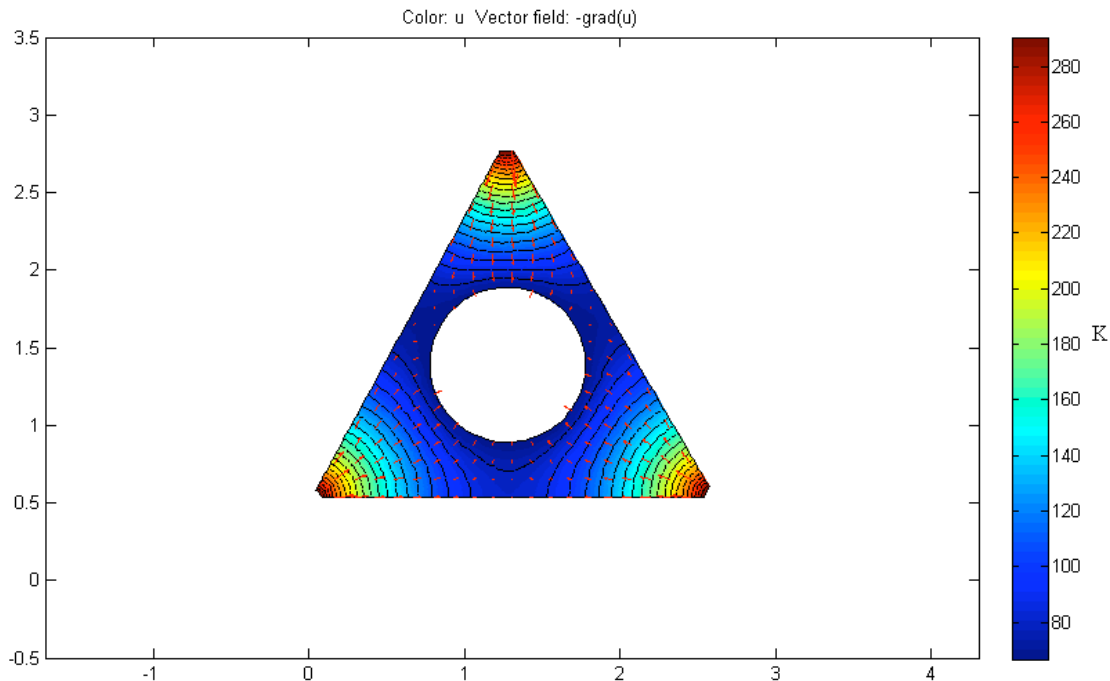

Fig. 5.10. Temperature distribution and heat flux across a Teflon support.

5.5.3. Results

In this analysis, the electrical power per meter was calculated for the models described with a spacing of 1 m between supports. Results are shown in Table 5.1. For the G-10 supports, the electrical power required by the refrigeration was about 6.0 W/m for both single stage and two-stage cooling. By using Teflon, the electrical power required by the refrigeration was 1.8 W/m for the single stage cooling and 2.1 W/m for two-stage cooling. For the stainless steel supports, the amount of electrical power for cooling the single stage was about 13.9 W/m. The electrical power for two stages of cooling was about 5.3 W/m.

Recall that these values are the upper bounds of the electrical power required by assuming perfect thermal contact between each support and the shells around it. However, this is not the case in practice. The realistic values are only a fraction of the electrical power for the perfect thermal contact case. Although we are uncertain of the actual electrical power requirement, we can still use the perfect thermal contact electrical power values to compare the two different models. To help compare these results, the values are normalized relative to the electrical power for G-10 single stage cooling.

Table 5.1.
Electrical Refrigeration Power for Cooling of Structural Supports.

	Electrical Refrigeration Power (W/m)			
	Perfect Thermal Contact		Normalized	
	Single stage	Two stages	Single stage	Two stages
G-10	6.0	6.0	1.00	1.00
Teflon	1.8	2.1	0.30	0.35
Stainless Steel	13.9	5.3	2.32	0.88

5.5.4. Summary

This works summarizes efforts to decrease the refrigerator power requirements for cryostats between room temperature and near liquid nitrogen temperatures. This work is relevant to systems operating at temperatures around liquid nitrogen, as well as to systems operating at lower temperature that use MLI thermal shielding between 66 K and room temperature.

It is shown that it is possible to decrease the electrical power requirements of the refrigerator for thermal radiation by about 38% by the use of a two-stage thermal shield, using refrigerator performance that is conservative, for a fixed total number of layers.

The thermal load was displaced from the 66 K refrigerator to the 160 K refrigerator by introducing an intermediate stage cooled by a separate refrigerator. The intermediate refrigerator had higher thermal loading because the number of shells in the gap facing

room temperature decreased relative to the case in only a single stage (16 layers vs. 32 layers). For this reason, the total electrical power was not reduced by as large of a factor as we had hoped, achieving only about a 38% reduction for the added complexity.

For thermal conduction, the electrical power of the refrigeration system can be decreased by about 60% by the use of a two-stage thermal shield with stainless steel supports. For G-10 and Teflon supports, it is shown that the electrical power of the refrigeration system remains the same by the use of a two-stage thermal shield.

In the perfect thermal contact case as described in the previous section, the radiation load and conduction load both contribute about equally. However, the realistic value for the electrical power is only a fraction (less than 1/3) of the perfect contact case. Also, if the spacing of the supports is more than 1 m then, the electrical power due to conduction could be further reduced. Therefore, it is reasonable to conclude that radiation is the dominant thermal heat path.

By combining the radiation and conduction analysis, it can be concluded that using Teflon structural supports and a two-stage thermal shield minimizes the electrical power requirement compared to the alternative combinations of the models discussed

6. Current Lead Optimization for Operation at Intermediate Temperatures

Current leads to low temperature environments represent a large heat input to the cryogenic environment. For cases that require large currents, such as in power distribution in intermediate voltages, the current leads represent, by far, the largest cryogenic thermal load and associated refrigeration requirement. Means of decreasing the refrigerator power when the cryogenic temperature is around liquid nitrogen temperature, or at temperatures that are optimized for high temperature superconductors, are discussed in this section The use of multiple cooling stages is described.

6.1. Introduction

For transmission applications, the losses in the current leads are small compared with distributed losses along the superconducting line which are dominated by thermal radiation (cryostat losses) and by the AC losses in the cable. Minimization of the current lead losses is not important. In these applications the lines operate at relatively high voltages and relatively low currents, compared with distribution cables.[3, 5, 16, 17]

In this work we are analyzing DC distribution, using HTS cables, in data centers. For this application, the use of relatively low voltages (~ 400 V DC) results in substantial currents to be distributed, on the order of 20 kA. Under these circumstances, current leads represent a substantial and dominant heat input to the cryogenic environment.

Means of optimizing current leads have been discussed in the past, mainly for applications to cryogenic environments around 4 K. Recently, the development of HTS current leads that can transfer currents between 77 K and 4 K have been developed with several companies selling commercial components. There has been little prior development of methods to minimize the heat input to the liquid nitrogen environment, as the requirements are significantly reduced compared with the more severe requirements to 4 K. However, in some potential applications, as in the data server or supercomputer centers, means of minimization of the cryogenic refrigeration load is desired.

In this section, the minimization of the refrigeration power for current leads between room temperature (298 K) and 65 K are discussed. The use of multiple intermediate stages is analyzed. This method has proven very useful to minimization of the cooling requirements when operating from room temperature to 4 K. [18]

6.2. Model

The methodology developed by McFee [18] has been used in this analysis. It provides a general methodology to optimize current leads, even with temperature dependent thermal and electrical properties.

The McFee formalism can be reduced to three equations. The minimum energy transmitted from temperature T_H to cold temperature T is given by

$$\dot{Q}(T) = I\left[2\left(\frac{k}{\sigma}\right)_{ku} (T_H - T) \right]^{\frac{1}{2}} \qquad (1)$$

and

$$\left(\frac{k}{\sigma}\right)_{ku} = \frac{1}{T_H - T} \int_{T}^{T_H} \frac{k(T)}{\sigma(T)} dT. \qquad (2)$$

where $k(T)$ and $\sigma(T)$ are the temperature dependent thermal and electrical conductivities of the conductor, and I is the transport current. The ratio of length to cross sectional area of the current lead that results in minimum thermal loss is given by

$$\frac{L}{A} = \frac{1}{I^2}\left[\sigma(T_L)[\dot{Q}_L]_{min} - \int_{T_L}^{T_H} \frac{d\sigma(T)}{dT} \dot{Q}(T)dT \right],$$

where T_L is the low temperature. Since $Q(T)$ is proportional to the current I by equation (1), the ratio IL/A is independent of current and only depends on the high temperature T_H, the low temperature T_L and the material properties of the current lead.

A case of special interest is the heat (and associated electrical power requirement for the refrigerator) that is transmitted from one temperature to another when a current lead

optimized for a given current is operated without current, such as during idle times of a magnet or no power transfer in a distribution or transmission line. Once the optimum *IL/A* is identified for a given temperature difference and material properties, the power transmitted from one temperature to the next when there is no current flowing is determined from

$$\dot{Q}(T_L)/I = \frac{\int_{T_L}^{T_H} k(T)\, dT}{I\, L/A}$$

It has been assumed that the current lead is made from copper with *RRR* =100. The assumed thermal and electrical properties of copper are shown in Fig. 6.1. It is possible to decrease the thermal load through the use of alternative materials for the current leads by about 10%, [19] but for simplicity copper is used in this study.
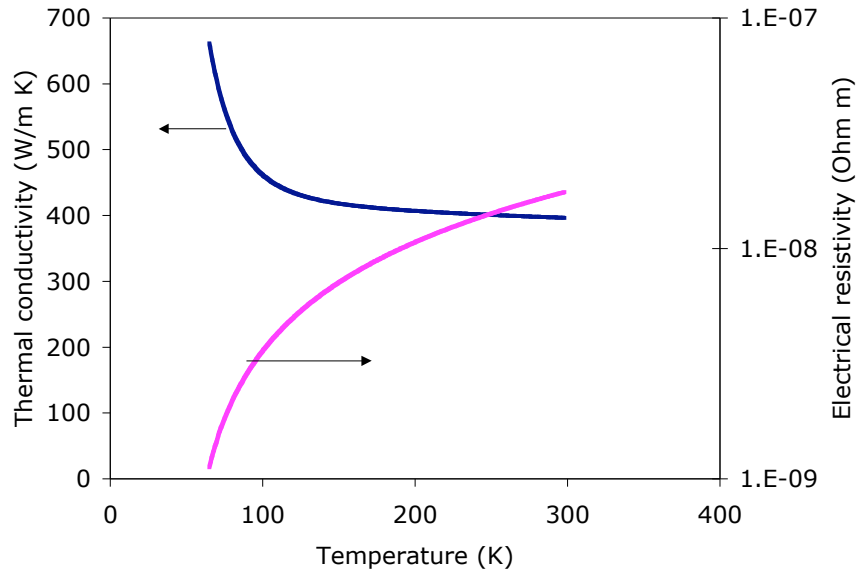

Fig. 6.1. *Assumed copper properties for the current lead with RRR = 100.*

In order to determine the electrical power requirement for the refrigerator system, an assumption needs to be made with respect to the efficiency of the refrigerators. In this work, it is assumed that the refrigerator efficiency is a constant fraction of the Carnot efficiency between room temperature and the operating temperature or the refrigerator. This is a simplifying assumption as the efficiency drops (compared with Carnot) for small capacity units and for lower temperatures. A relatively conservative multiple of 9 (i.e., 11% of Carnot efficiency) is used in Section 3 for all refrigerators, independent of temperature and capacity.

The normalized electric power requirement for an individual refrigerator P_E is thus,

$$(P_E/I) = 9\,(Q/I)\,/\eta_{Carnot}$$

where $\eta_{Carnot} = T_L/(T_H - T_L)$ is the Carnot efficiency of the refrigerator operating between upper temperature T_H and lower temperature T_L. The total electrical power is the sum of the electrical power of the individual refrigerators.

6.3. Copper Lead Optimization

The power requirement has been calculated for three cases when the leads are manufactured from copper: a single stage current lead (cooling only at the operating cryogenic temperature), one with cooling at an intermediate temperature, and finally one with two intermediate cooling temperatures. The temperature of operation has been varied in the second and third cases such that the total electrical power of the refrigerators is minimized.

The minimization function is the electrical power. Alternatively, the minimization function could be the capital cost of the overall refrigeration system, or the cost of ownership (capital and operating costs).

Figure 6.2 shows the results of the calculations for the single stage, two-stage and three-stage current leads. The calculated normalized electrical power P_E of the refrigerator or refrigerator set, assuming the model described in the previous section, are shown as a function of the lower temperature of the upper stage (first stage), for two-stages and three-stages systems. Also shown in the normalized electrical power for the single stage. For the single stage case, the normalized electrical power is 1.36 W_E/A, (W_E is electrical Watt) which decreases to about 0.92 W_E/A for two stages, for a one third reduction of electrical power. The gain of going from two-stages to three-stages is minimal, with an additional electrical power reduction of about 6%.
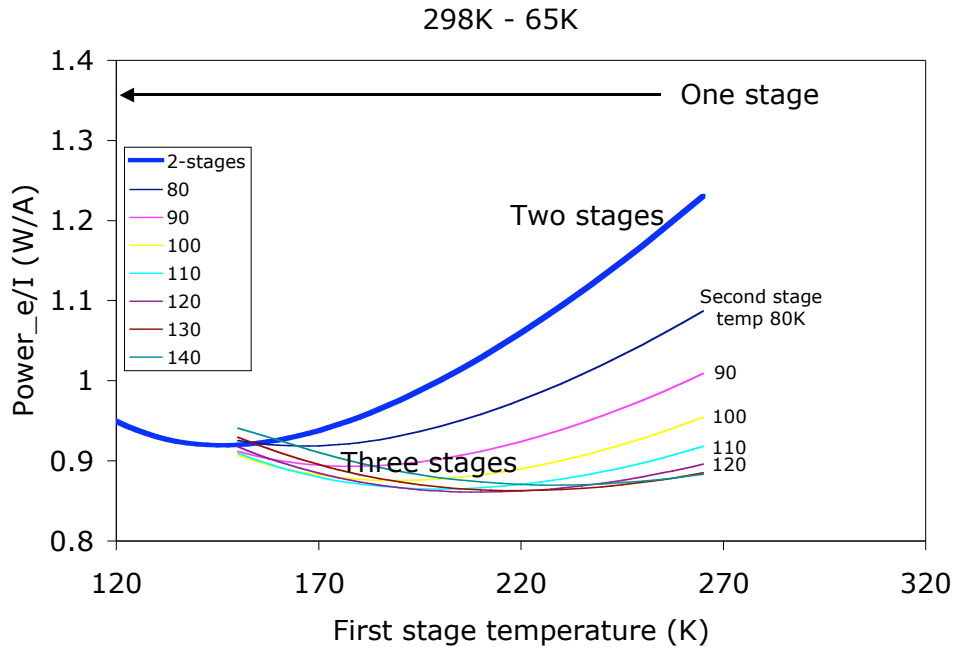
Fig. 6.2. Normalized refrigerator system electrical power as a function of the temperature of the intermediate stage for two and three stage refrigeration systems.

The case of two-stages has a broad optimum around an intermediate temperature of 145 K. At this temperature, the normalized thermal input at the first (145 K) and second (64 K) stages are 0.039 and 0.017 W_T/A, respectively. The corresponding electrical power of the respective refrigerators are 0.37 and 0. 55 W_E/A.

The corresponding values of *IL/A* at the electrical power minimum are 3.7 10^6 A/m for the single stage case, and for the two stage current lead, *IL/A* ~ 2.83 10^6 A/m for the high temperature side and 1.48 10^6 A/m for the low temperature side.

Fig. 6.3 shows the value of *IL/A* required for the single and two stage current leads, as a function of the cold stage temperature. Note that the overall values of *IL/A* for the two stage current lead is about double that of the single stage current lead.
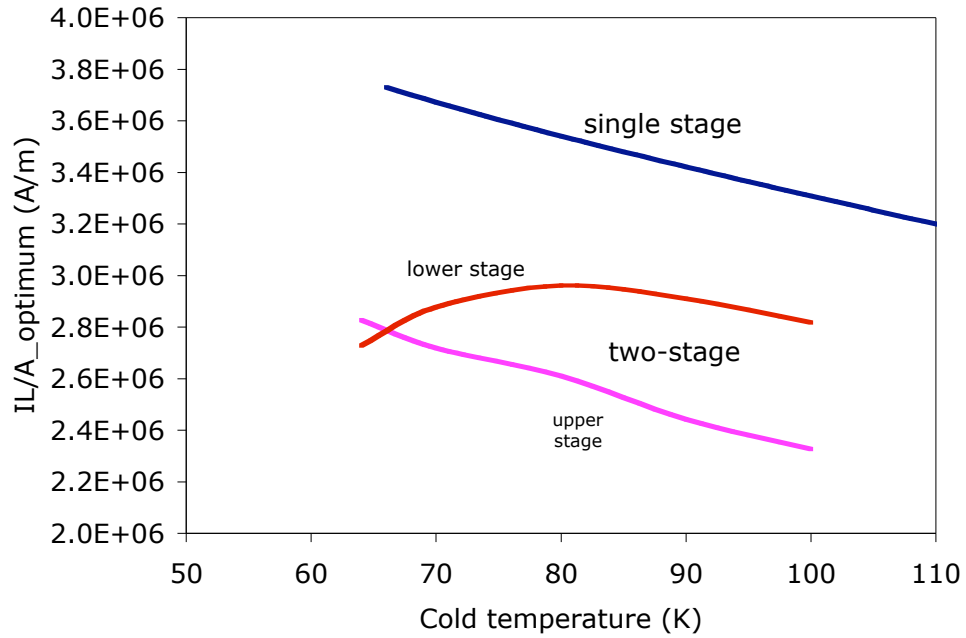
Fig. 6.3. Values of IL/A for optimized single-stage and two-stages current leads.

The properties of the optimized current leads, including the thermal loading in the case of no current, are shown in Table 6.1 for both the single and two stage current leads.

Table 6.1.
Characteristics of the optimized single and two stages current lead

| | | Single stage | Double stage | |
			Upper stage	Lower stage
Q_dot	W/A	0.042	0.039	0.017
IL/A	A/m	3.73E+06	2.83E+06	2.73E+06
Q_dot no current	W/A	0.027	0.022	0.014
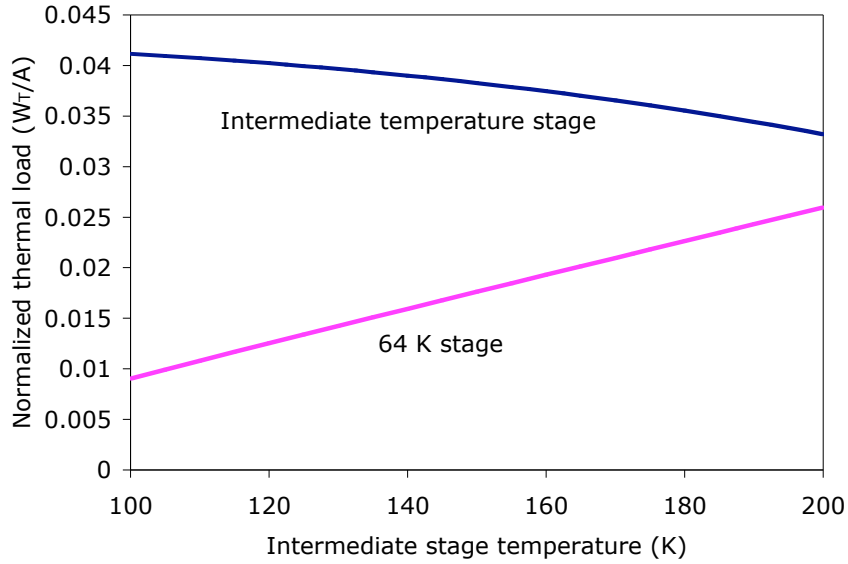
Fig. 6.4. Normalized thermal loads at the 64 K and intermediate-stage temperature as a function of the intermediate temperature, for optimal individual leads

It is interesting to note the thermal power loading at the different temperatures. For the case of two stages, the power loading at the 64 K station and at the intermediate temperature stage is shown in Fig. 6.4 as a function of the intermediate stage temperature. As the temperature of the intermediate stage increases, the individually optimized thermal loading to the upper stage decreases while the thermal loading to the lower stage increases. At the system optimum intermediate temperature (around 145 K as shown in Fig. 6.2), the thermal loading to the low temperature is slightly less than half the thermal loading of the intermediate stage. At this optimum, the electrical power of the 64 K temperature refrigerator is, however, about 50% larger than that of the intermediate temperature refrigerator.

Table 6.2.
Characteristics of optimized current leads with two stages as a function of the lower temperature

		64	70	80	90
Lower temperature	K	64	70	80	90
Intermediate temperature	K	145	155	165	180
Upper stage					
Q_dot	W/A	0.039	0.038	0.037	0.036
IL/A	A/m	2.83E+06	2.72E+06	2.61E+06	2.44E+06
Q_dot no current	W/A	0.022	0.021	0.021	0.020
Lower stage					
Q_dot	W/A	0.017	0.018	0.020	0.022
IL/A	A/m	2.73E+06	2.88E+06	2.96E+06	2.91E+06
Q_dot no current	W/A	0.014	0.014	0.013	0.014

Table 6.2 shows the results of the calculations for the two-stage system as a function of the cold temperature. The system performance has been evaluated for cold temperature of 64K, 70K, 80K and 90K. The associated value of the intermediate temperature that minimizes the electrical power consumption of the refrigerator system is shown to increase faster than the cold temperature.

Also shown in Table 6.2 are the system-optimized values of the normalized heat flow when operating at full current and the associated value of *IL/A* of the optimized system. Table 6.2 shows these values for both the upper stage and the lower stage. The impact on the system of operating without current, especially during extended periods, as in cases where a load such as a bank of computers in the data center have been disconnected, as also shown in Table 6.2 for the case of optimized two-stages current lead.

6.4. Non-Copper Current Leads

It is well known that it is possible to decrease the thermal loading with single stage current leads through the use of materials other than copper. In particular, aluminum leads have about 10% lower thermal loading for single stage. In this section, the possibility of using multiple materials in different sections of the current lead is discussed, and the optimized parameters for multiple stage non-copper leads are presented.

Using the formalism by McFee, from equation (1) it is easy to see that for a given temperature span, the thermal loading is minimized for those materials with the lowest ratio between thermal and electrical conductivities. Figure 6.5 shows the parameter k/s as a function of temperature for 4 different materials: copper (as in the previous section), and three aluminum alloys: 1100, 5083 and 6061.[20, 21]
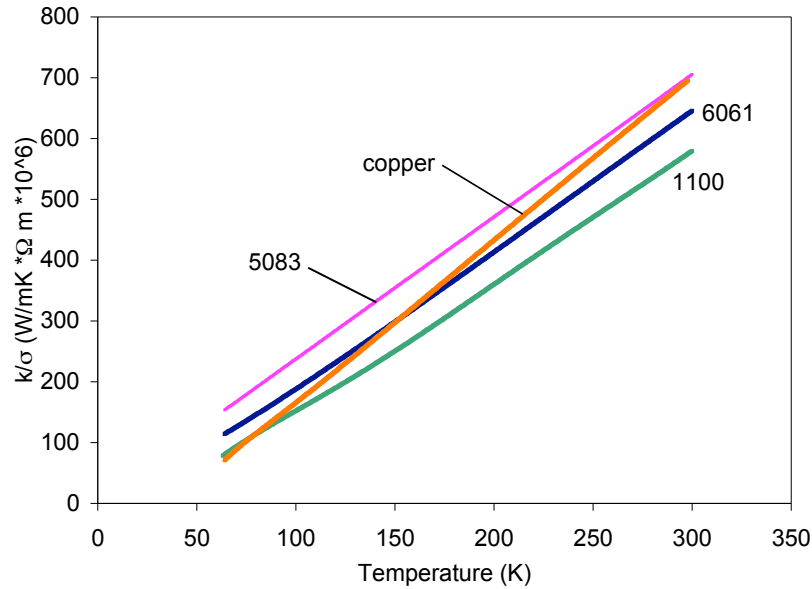
Fig. 6.5. Ratio of thermal to electrical conductivity for copper and several aluminum alloys as a function of temperature.

From Fig. 6.5, it is clear that over the entire span, with the exception of a very small region near 65K, the use of 1100-series aluminum minimizes the thermal loading, for any temperature span and irrespective of the number of stages. In the rest of this section, the implications of using one and two stages with 1100 series aluminum is presented.

Table 6.3 shows the results from the optimization of a single stage and two-stages current leads, between 298 K and 65 K. The intermediate temperature of the optimum system has increased to about 150 K. As in the case of copper, the optimum is quite broad. The two-stage system decreases the electrical power requirement by about 1/3.

Table 6.3.
Optimized current leads with 1100 series aluminum

		Single stage	Two stages
Intermediate temperature	(K)		150
		Upper stage	
Q_dot/I	W/A	0.039	0.035
IL/A	A/m	2.18E+06	1.62E+06
Q_dot/I no Current	W/A	0.024	0.020
		Lower Stage	
Q_dot/I	W/A		0.017
IL/A	A/m		1.85E+06
Q_dot/I no Current	W/A		0.011
P_e/I	W/A	1.278	0.867

37

6.5. Summary

This works summarizes efforts to decrease the refrigerator power requirements for current leads operating between room temperature and near liquid nitrogen temperatures. This work is relevant to systems operating at temperatures around liquid nitrogen, as well as to systems operating at lower temperature that use low-thermal conduction HTS current leads, as the overall electrical power requirement of these current are dominated by the stages between room temperature and around 70K.

It is shown that it is possible to decrease the electrical power requirements of the refrigerator by about 1/3 through the use of two-stages current leads, using refrigerator performance that is conservative. With real systems, with higher temperature refrigerators running at higher fractions of their Carnot efficiencies, it is suggested that the refrigerator electrical power requirement can be decreased by 1/2.

Not analyzed in this document is the impact of the optimization on capital cost, or, more importantly, on the cost-of-ownership. Only the electrical power requirement was minimized. The higher temperature refrigerators are cheaper that comparable low temperature refrigerators, but the fact that each individual refrigerator of a multi-stage unit has smaller capacity increases the cost per unit (refrigerators show a decrease in cost per watt that scales as $C^{-0.3}$ where C is the capacity of the refrigerator).

We are starting a compilation of state-of-the-art cryogenic refrigerators in order to provide information required in order to repeat the exercise for capital cost minimization as well as operating cost minimization using realistic temperature/capacity dependence of refrigeration efficiency.

7. Cooling Topologies for Superconducting Power Systems: I. Short Distance Electric Distribution

In this section the topologies for cooling superconducting cable systems are investigated. The goal is to explore options that allow for flexibility of operation, low temperature rise in the superconductor and low refrigerator power consumption. A focus of this section is the study of means for cooling distribution systems with cryogenic loads dominated by current lead loss. Use of multiple fluids to decreased the refrigerator power requirements are described, and potential alternative candidate fluids are proposed.

7.1. Introduction

Short distance distribution systems have characteristics that make them very different from long-distance transmission lines. One of the main differences is that the cryogenic

loads are dominated by the current leads losses, as opposed to long-distance transmission lines, where the heat load is dominated by distributed losses due to the cryostat. A second difference is that the short distance grid may be characterized by a large number of secondary feeders along the distribution line, as opposed to transmission, where there is a small number of feeders, or only terminations at each end.

There are two possible coolants of interest for cooling superconducting distribution lines: liquid nitrogen (subcooled), and gaseous helium. Liquid nitrogen has the advantage of much smaller temperature rise in the coolant for a given volumetric flow, but it is limited in the minimum temperature where it can operate, at around 65K. Gaseous helium is not limited by the temperature for expected temperatures of operation of the SC distribution grid, but it requires much larger volumetric flow rates. It requires comparable mass flow rates to liquid nitrogen, but since gaseous helium has much lower density, the corresponding volumetric flow rates and the operating pressure drops are higher. The high flow rates result in increased pressure drop, and the changes in density with temperature are much larger than for liquid nitrogen.

There is a substantial literature on the minimization of the cryogenic load on conduction-cooled current leads, starting with the work of McFee.[18] Iwasa has systematically reviewed work on this field.[22] Recently, there has been work to try to minimize further the cryogenic load. Yamaguchi has proposed and tested the use of Peltier elements at the high temperature side of the current leads.[7] Bromberg has optimized the use of intermediate temperature stages as further means of decreasing the cryogenic load.[23] These studies indicate that it may be possible to decrease the cryogenic load by about half that of conventional systems.

In the case of current leads, the refrigeration requirement is about 0.1 W/A per current lead pair, for currents that go from room temperature to approximately liquid nitrogen temperature Depending on the voltage of the transmission line, the cryogenic requirement for the primary feeder current leads could be as high as 2.5 kW (for 25 kA SC bus, 400 V), per set of power leads. A similar loss occurs in the secondary spurs (as the integrated current of the secondary spurs is the same as that of the primary feeders). The secondary spurs result in distributed losses along the distribution line. These large cryogenic loads represent a challenge. For one, it would be best if the superconductor temperature is as low as possible in order to minimize the amount and cost of superconductor required. Superconductor cost minimization is very important, especially in the near and middle term. The cost of the superconductor is a substantial fraction of the cost of the system, and thus its performance needs to be maximized.

In this document a few approaches that address the unique cooling needs of superconducting distribution systems are investigated. In particular, DC systems are investigated.

7.2. DC Distribution System Characteristics

Figure 7.1 shows a superconducting DC distribution system, such as those proposed for a data center.[24] With respect to Fig. 7.1, the power may come to the site through a high voltage transmission line, and then it is reduced to low voltage by an onsite transformer (not shown). The AC power output from the AC transformer is converted to DC by an AC/DC converter, followed by an uninterruptible power supply (UPS).   The uninterruptible power supply can be a SMES, capacitors, ultracapacitors, battery, diesel generator set with AC/DC conversion, or other. A set of current leads, 8a and 8b are used to introduce the current to the superconductor through the cryostat. A large number of spurs 12 provide connectors to the superconducting distribution bus 9 (composed of elements 9a and 9b). Some of these spurs may be terminated by terminations 13, within the cryostat, that are not active in order to provide flexibility to the distribution bus. Most of the spurs are active and connected to current leads 10 that transfer the current from the superconductor to a normal conductor through the cryostat. These currents power the loads. The current is then returned by a similar superconducting electrical distribution bus.
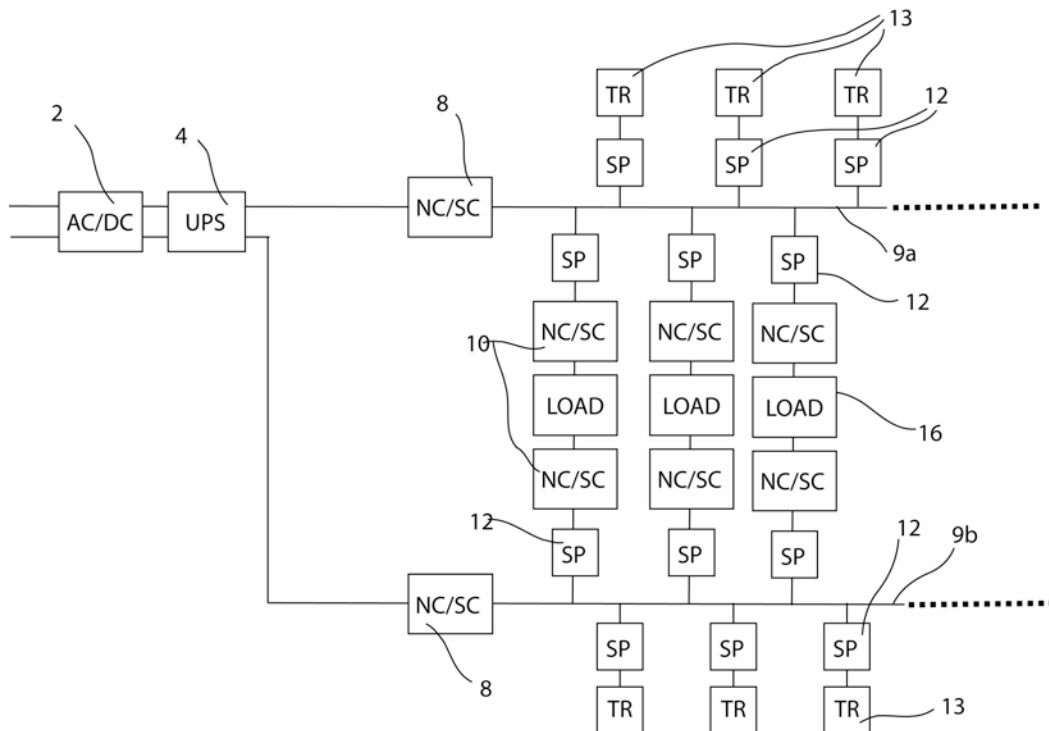

Fig. 7.1. Schematic diagram of a circuit for a superconducting DC distribution system. Labels are defined in the text.

For DC distribution, it is desirable to have the current return also be at voltage, in order to maximize the transfer of power for a given amount of superconductor.   If this arrangement is chosen, then the voltage polarity of bus 9a and 9b are opposite. In order to tolerate unbalanced loads, faults, or transients, a small ground return is needed (not shown). This approach is attractive when the transmission is at high voltage, as the voltage is halved for constant power delivery capability.

Table 7.1 shows rough numbers for the cost of a nominal 10MW system for a data center with a topology as shown in Fig. 7.1, with large power-density requirements.[8]   The numbers from the Navigant study have been used to scope near, middle and long-term costs, assuming trends in cost reductions for the superconductor, the refrigeration units (cryocoolers), and the cryostat. [11] It is not intended that Table 7.1 be precise, but rather to point out the items that dominate the cost. It is assumed that the distribution line operates at 400V and is 200 m long.

Table 7.1
Costs of SC distribution system for data center

Power	MW	10	10	10
Length	m line	200	200	200
Voltage	V	400	400	400
Current	A	25000	25000	25000
YBCO cost	$/kA m	$400.00	$50.00	$10.00
Total cost		$4,000,000	$500,000	$100,000
Cost of cryostat	$/m	$500	$300	$100
		$200,000	$120,000	$40,000
Cost of cryocooler	$/W	$100	$60	$25
Heat leat	W/A	0.2	0.1	0.1
Total heat leak	W	5000	2500	2500
Refrigerator cost		$500,000	$150,000	$62,500
Refrigerator power	W at RT	50000	25000	25000
Total cost		**$4,700,000**	**$770,000**	**$202,500**

It is clear from Table 7.1 that in the near term the cost of the superconductor dominates by a wide margin. In the longer term, the cost of the cryogenic system is comparable to the cost of the superconductor. The reason for the relative change of the costs is that it is expected that the cost of the superconductor, a recent technology, will experience much faster cost reduction than either the cryostat or the cryocoolers, which are more mature technologies.

It is assumed that the cryogenic heat load is dominated by the current leads, which is a good assumption for short length cryostats. Means are being investigated in this report to decrease the thermal load due to the current leads and to investigate means to minimize the temperature rise in the superconductor coolant.

7.3.   Topology Options for Cooling the Superconductor and the Current Leads

The cooling process for a superconducting power distribution network requires special attention, different from superconducting power transmission lines where distributed

losses along the cryostat dominate. In the case of short distribution networks the lumped losses due to the local heating by current leads dominate the refrigeration requirements. This is especially true of the case when the superconducting distribution system has current leads for the primary and secondary feeders, and less of an issue for the case when there are not leads and the power transfer occurs via transformer action, which requires AC. Another difference between the superconducting distribution line and the superconducting transmission line is the use of many secondary feeders, although both lines utilize a single or a small number of primary feeders. The topology of the cooling geometry needs to address the following loads:

- Current lead
- Cryostat heat loads
- Superconductor losses

As mentioned above, it is ideal to have the superconductor as cold as possible. The cryostat and the current leads can have substantial temperature rise without major impact to the performance of the superconducting cable. Thus, it may be possible to cool the current leads separately from the superconducting cable, allowing the temperature of the cold end of the current lead to rise above the temperature of the superconductor. It may be necessary to decrease the current density in the transition from the normal current lead to the superconductor, and there will be heat conduction to the main superconducting cables. However, the temperature difference is expected to be small and thus the impact on the cryogenic losses is not large.

For DC application, the superconductor losses are negligible. Thus, only the cryostat losses and the current leads need to be addressed. For some of the best cryostats, it has been determined that the losses per unit length (due to radiation, conduction and convection) are around 1-2 W/m. For this system with 400 m of cryostat (for both polarities of a DC system 200 m long), the cryostat losses are small (see Table 7.1). It will be assumed that the approach of Bromberg[25] will be used, minimizing the heat into the low temperature environment to 0.1 W/m.

Figure 7.2 shows a schematic of the conventional approach [3, 26, 27], with a single coolant that cools simultaneously the superconductor, the cryostat, and the current lead of a spur along the line.
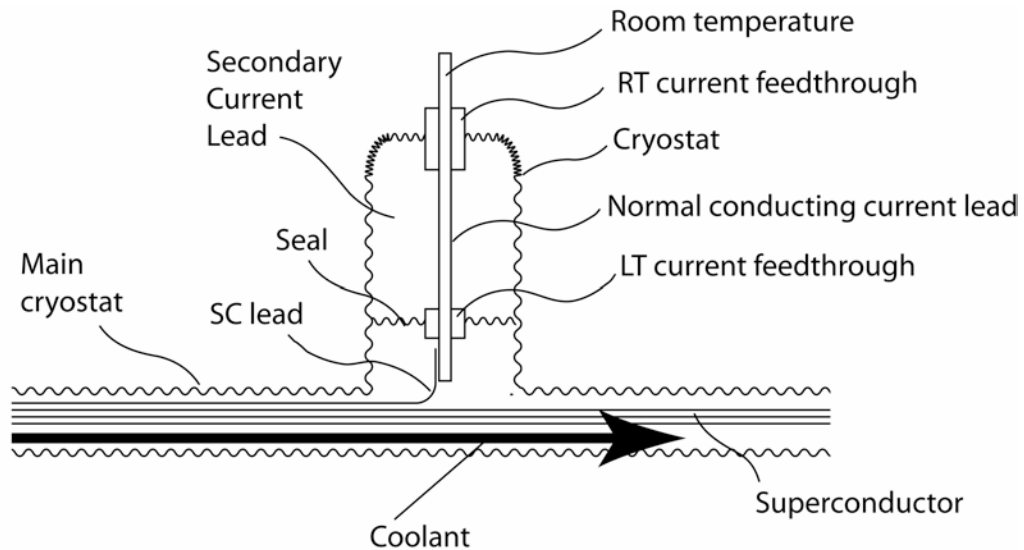
Fig. 7.2 Conventional approach for cooling superconducting bus and current leads

In Fig. 7.2, a current feedthrough and seal separates the coolant from the uncooled region of the current lead. The current lead consists of a cryostat that is shown in simplified form in Fig. 8.2, a normal element, and a superconducting element. A superconductor to normal conducting material joint is made between the normal conductor and superconductor lead in the cooled section of the cable. The normal conductor leaves the cryostat region through a current feedthrough. This geometry has the disadvantage that the heated coolant is remixed with the cold nitrogen. The superconductor downstream from the lead experiences increased temperature and thus decreased current carrying capability. High coolant speeds and large excess coolant capability can be provided to avoid this problem. In the case of excess coolant capability, the temperature differential between the cable inlet and the cable outlet are small, but there is increased pressure drop across the coolant loop with decreased pressure at the cable outlet (for a given inlet pressure).

With these constraints, it is possible to conceive multiple topologies that satisfy the requirements. The main constraint is that the superconductor has to be cooled with a separate fluid (or upstream using the same coolant) from the coolant that cools the current leads.
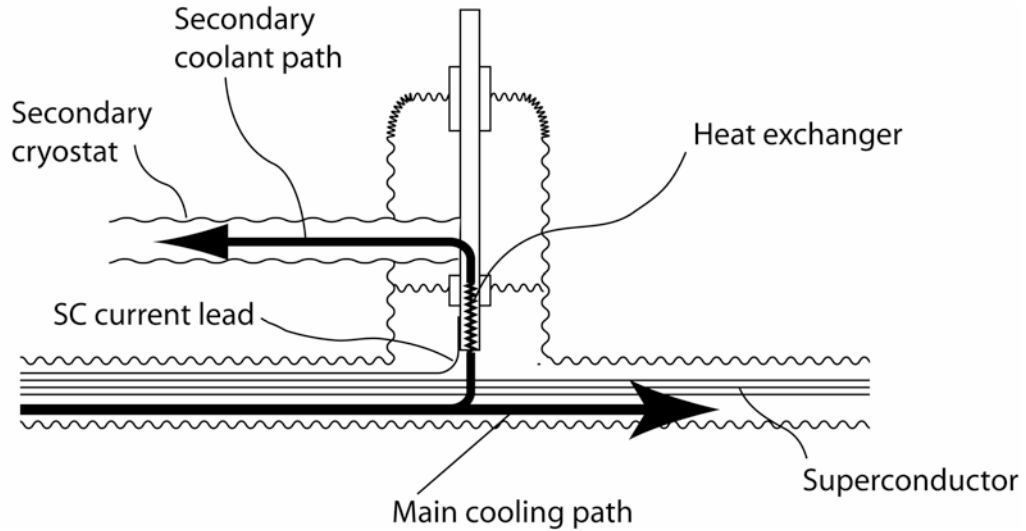
Fig. 7.3 Cooling topology with segregation of the coolant fraction for cooling the secondary feeder current lead (a single spur is shown) away from the superconducting bus.

Figure 7.3 shows a topology with the coolant that is used to cool the current lead extracted from the cold coolant stream, reducing the heat ingress into the superconductor coolant. A fraction of the main coolant is used to cool the current lead through a heat exchanger, and the warm coolant is removed from the cold cryostat and returned through a separate coolant channel. It should be noted that the two separate coolant paths can be within the same cryostat, to minimize the cost of the cryostat.[25] Multiple current leads can be cooled in this manner, with the return path of the warm coolant returning through a single path towards the inlet of the cold coolant. One advantage of this geometry is that the coolant is returned to the inlet, where it can be recooled and reused for the inlet.
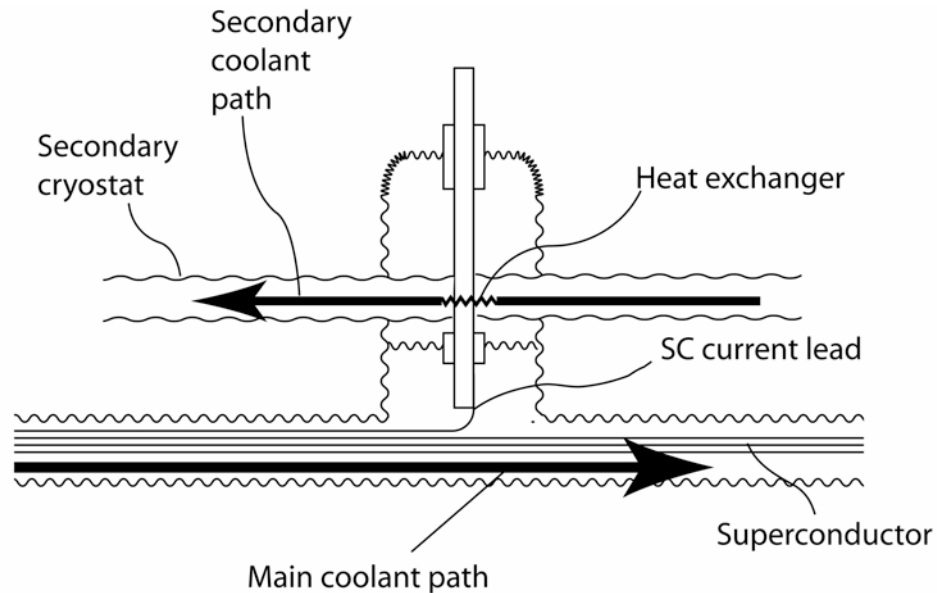

Fig. 7.4. Cooling topology with separate cooling paths for the superconducting bus and for the secondary feeder (a single spur is shown) current leads

44

Figure 7.4 shows a variation of the topology shown in Fig. 7.3, where there are two separate cooling paths that cool the arrangement, with the cold coolant path only cooling the superconductor bus, and the second, warmer coolant loop cooling the current lead. Note that there is distance along the normal conductor between the region cooled by the warm coolant and that by the cold coolant. The temperature difference between the two regions along the normal conductor results in heat transfer to the cold path, but, because ΔT is designed to be small, the heat input is small. Although shown in separate cryostats, it is possible for both paths to be in the same cryostat.

There is an operational difference between the topologies shown in Fig. 7.3 and Fig. 7.4. In Fig. 7.3, the current leads of the spurs are all cooled with basically the same temperature coolant, as the heating of the superconductor is small. In Fig. 7.4, the temperature of the coolant increases downstream from the current lead coolant, as there is substantial heating of this flow. However, there is simplicity in the manifolding of Fig. 7.4 as there are only two main flows in the system, as opposed to multiple flow paths in the case of Fig. 7.3.
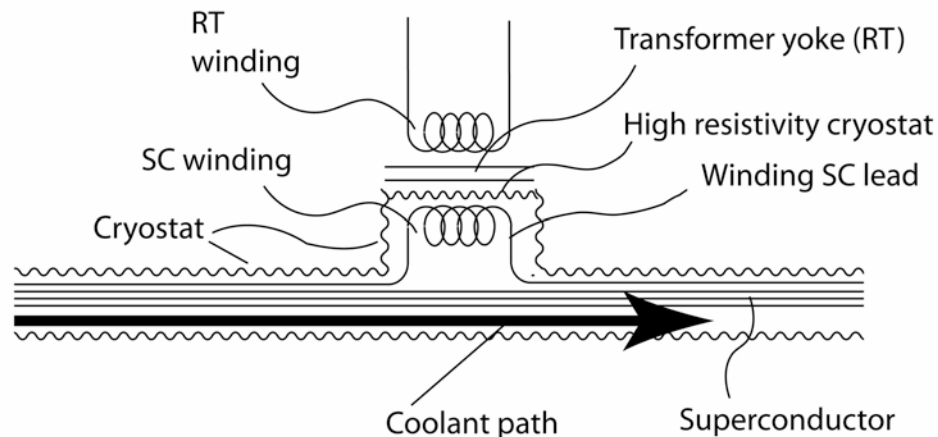

Fig. 7.5. Coolant topology of contactless current transfer, with a single coolant path (for AC operation only).

7.4. Fluid Options for Intermediate Coolants

The use of intermediate coolants can be used to minimize the electrical refrigerator requirement. Bromberg analyzed the effect on the current leads[23], while Miles investigated the effect for the cryostat.[28]

There are several fluids that can be used as intermediate coolants. Some of the most promising fluids are shown in Table 7.2, which compares the properties of these fluids, including boiling temperatures at 1 bar and at 10 bar, the heat capacity, density, and temperature excursion to the boiling phase between 10 bar and 1 bar and the heat capacity over that excursion. A figure of merit can be determined by dividing the rate of heat removal capability, $c \rho \Delta T A V$ (where c is the heat capacity, ρ the density, ΔT the

allowable thermal excursion, A the cross sectional area of the channel, and V the velocity of the fluid), by the pressure drop per unit length, f /2 (where f is the friction factor). Although the figure of merit could have been the rate of heat removal divided by the pumping power, it is determine that the pumping power is not large, and thus not important, but the pressure drop limits the window of operation. Two assumptions for the friction factor were made in Table 7.2, one for laminar flow and the second one for turbulent flow. In laminar flow, $f \sim 1/Re$, where Re is the Reynolds number, and the figure of merit reduces to $c \rho \Delta T A D / \nu$, where D is the diameter of the cooling passage and ν is the viscosity. For the case of turbulent flow, f is only weakly dependent on Re, and the figure of merit is $(c \Delta T) A / V$. Table 7.2 shows the figures of merit for the different coolants considered, for constant A and constant V (for the case of turbulent flow).

The light hydrocarbons are about a factor of 2 better than liquid nitrogen. For the hydrocarbons, the boiling temperature is lowest for methane, and increases with molecular weight. Ammonia shows a high performance, but its temperature is rather elevated. However, the use of any of these coolants requires a more complex cryogenic system, with multiple coolants.

In this report, the possibility of using a second liquid nitrogen coolant path, operating at higher temperature is investigated. The implications for cooling the leads for distribution systems, as well as cryostat losses for transmission systems will be discussed in the following sections.

Table 7.2.
Properties of potential cryogenic fluids

	Boiling 1 bar K	Boiling 10 bar K	ρ kg/m^3	ΔT K	c kJ/kg K	viscosity microPa s	visc average microPa s	$c \rho \Delta T / \nu$	$c \Delta T$
Nitrogen	77	105	750	30	2.2	130	130	381	66
Ammonia	240	300	650	60	4.3	500-150	300	559	258
NF3	170	220	1500	50	1	???	300	250	50
Methane	110	150	400	40	3.5	100-50	75	747	140
ethane	180	250	500	70	2.3	150-100	120	671	161
Propane	215	300	600	60	2	500-150	300	240	120
Argon	90	118	1300	30	1.2	120-200	150	312	36

7.5. Calculation of Performance of Cooling Topologies for Distribution Systems

In this section, the performance of the several options discussed in Section 3 is assessed. It is not the goal of these calculations to fully optimize the system, as much more work needs to be done, including detailed investigation of the performance of the refrigerators. Instead, the goal is to provide insight into the potential advantages of the different options.

The calculations have been performed for a DC distribution grid, such as for a data center. For the purpose of the illustration, it is assumed that the total current is 25 kA and the length of the cables is 200 m. It is the goal of the design to limit the temperature excursion of the superconductor, since as shown in Table 7.1 it dominates cost in near term implementations. It is also desirable to minimize the power requirements for the refrigerators.

For the studies, a compressible, steady state code has been used (CCAN), developed at MIT by Gierszewski.[29] CCAN calculates the temperature, pressure, power, and other engineering quantities along the length of an actively cooled electrical conductor. The code was developed to perform engineering analysis of internally cooled conductors. The code assumed single-phase flow and neglects axial conduction relative to heat transfer to the coolant. It is assumed that the refrigerators operate with 1/9 of Carnot efficiency, corresponding to near term expectations from the Navigant study.[11]

For this application, the cryogenic loads are dominated by the current leads. Table 7.3 shows the relevant parameters of the system. It is assumed the cryogenic load per each current lead is 0.05 W/A, a value that represents the state-of-the art. Bromberg has performed calculations to determine the optimization of current lead design using intermediate cooling, which could substantially decrease the cryogenic load to the cryogenic environment.[23] It is assumed that the system does not provide current path redundancy of the secondary system. If it does, the cryogenic load would increase by about a factor of 1.5 for a second set of current leads that are not carrying current, but result in increased cryogenic load. The cryogenic losses in the distribution system are indicated in Table 7.3, excluding those of the terminations (which could be cooled separately). In addition, only one of the polarity losses is described. Thus, only about 1/4 of the total cryogenic loads are included. However, these loads are distributed, and it is the purpose of the present report to investigate means of cooling them.

Table 7.3.
Parameters for Superconducting DC distribution in data centers

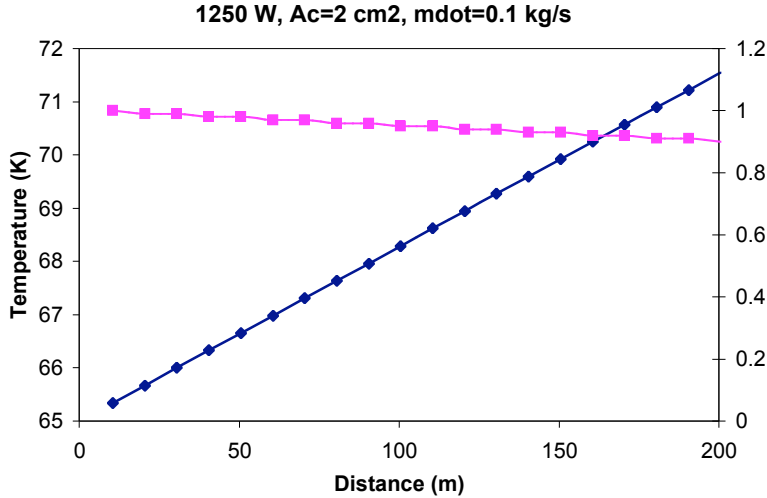|		
Length	m	200
Current	A	25000
Cryogenic load	W/A	0.05
Total load, cable	W	1250
Cryostat load, Low T	W/m	0.1
Refrigerator efficiency		1/9 of Carnot

Fig. 7.6. Temperature and pressure along the length of a conventional data center SC distribution system (as shown in Fig. 7.2).

Figure 7.6 shows the temperature and pressure along the distribution system, for conventional current leads, assuming that the current leads in the secondary system are distributed uniformly along the length of the cable. Because of the relatively short length (200 m), the pressure drop is not a problem, in sharp contrast with long-distance transmission systems (described in an accompanying report).[25] Substantial flow rates can be provided, 0.1 kg/s, in small cross sectional area (2 cm^2), with relatively small pressure drops. All of the heat is being removed at the low temperature.

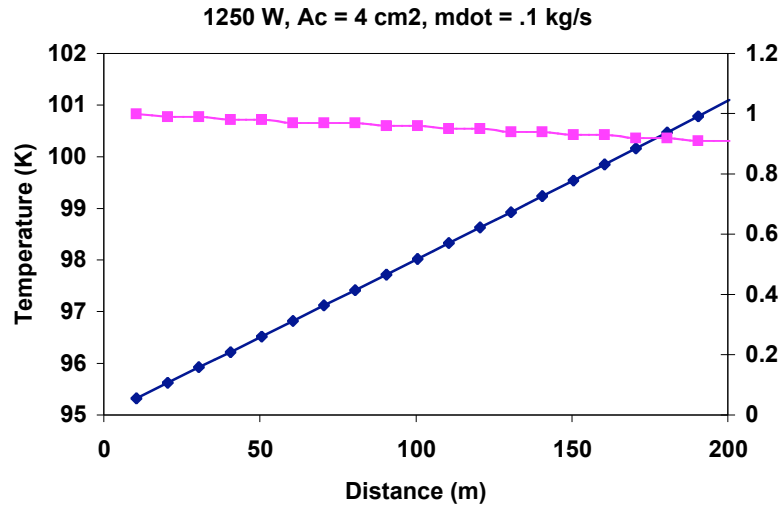**1250 W, Ac = 4 cm2, mdot = .1 kg/s**

Fig. 7.7. Temperature and pressure along the distribution system for the current lead cooling paths shown in Fig. 4, operating near 100 K

Figure 7.7 shows the results for the case when the current leads are cooled separately, and the heat is intercepted at around 100 K. The result of this case is to minimize the cryogenic load to the low temperature environment.

Finally, the results of a system where the coolant first cools the superconductor and then the current leads, as in Fig.7.4, are shown in Fig. 7.8. The total length of the coolant path in this case is now 400 m. The cross section of the coolant is decreased, as there is larger temperature drop allowed for the coolant in the return path since it is not affecting the superconductor. The coolant flow rate has also been decreased, to 0.02 kg/s, resulting in a much larger temperature rise in the coolant. The high temperature occurs in the return path when the coolant is used to cool the current leads, not the superconductor (as shown in Fig. 7.4). The system has been sized so that the temperature at the outlet is near 100 K, near the boiling point. There is single-phase fluid through the entire length. In this case, it is assumed that the cold environment experiences a heat loss of about 1/20 that of the case when the current leads are cooled by the cold coolant.

The comparison between the three approaches is shown in Table 7.4.   Included in this table are the refrigeration loads. There is a substantial benefit from cooling the current leads at the higher temperature (intercepting the heat at higher temperature, resulting in substantial decrease of power requirement for the refrigerators). The savings in the coolant are about 35% for the case of separate coolant (Fig. 7.4, with a return path cooling the current leads at a relative high initial temperature) and 15% for the go-and-return case (with a return at the initial temperature of the superconductor).

Table 7.4.
Comparison between base case (Fig. 7.2), separate coolant (Fig. 7.4) and go-and-return.

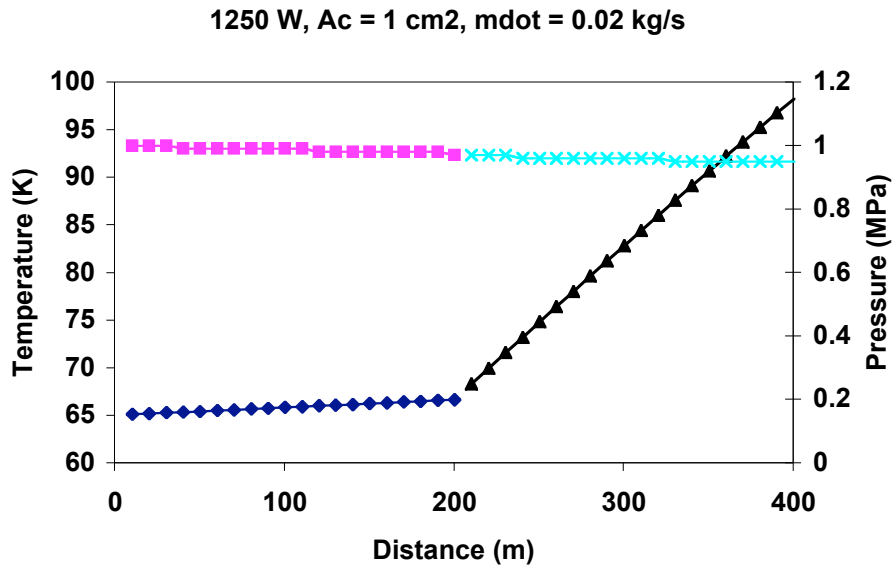|		Base case	Only current lead	Go and return Low T	High T
Distributed load, total	W/m	6.26	6.26	0.31	6.26
mdot	kg/s	0.1	0.1	0.02	0.02
Ac	cm^2	2	2	1	
Tinlet	K	65	95	66	67.7
Texit	K	71.5	101	67.6	98.7
pexit	MPa	0.9	0.91	0.97	0.94
Refrigerator power	kW	21.5	13.1	1.1	17

1250 W, Ac = 1 cm2, mdot = 0.02 kg/s

Fig. 7.8. Temperature and pressure along the length of a SC distribution system, where the coolant first cools the superconductor, and the current leads.

7.6. Heat Exchanger Considerations

Even in the case of liquid coolant, substantial cross sectional area may be required in order to transfer the heat from the current leads to the coolant. For the case of secondary feeders, areas on the order of 1000 cm^2 and coolant flow speeds of 0.10 m/s are sufficient. For the primary feeder, carrying much more current, it is necessary to develop a heat exchanger that includes about the same area but much higher liquid nitrogen flow speed, on the order of meters per second. As the length of the heat exchanger is not large, the associated pressure drops are small. Thermal anchors at the cryogenic temperature with multiple holes or fins for increased cooling are desired. In both cases, the flow of the liquid nitrogen is in the direction from the superconductor to the copper in the current lead.

7.7. Summary

In this report, several topologies for cooling superconducting distribution systems have been explored. The possibility of separating the cooling of the superconductor from that of the current leads has been explored.

It has been determined that the most attractive topologies include a separate cooling of the current leads, operating near the boiling temperature of the coolant, high-pressure nitrogen. The superconductor is cooled through a separate path, using much colder coolant, with minimum temperature rise. The solution results not only in an attractive solution for cooling the superconductor and the current leads, but also in substantial reductions of the refrigerator power requirement and minimizing the use of expensive superconductor.

8. Cooling Topologies for Superconducting Power Systems: II. Long Distance Electric Transmission

In this section the topologies for cooling superconducting systems are investigated. The goal is to explore options that allow for flexibility of operation, low temperature rise in the superconductor and low refrigerator power consumption. Here we explore means of cooling the cryostat in a long-distance electric power transmission systems. Use of multiple fluids or multiple coolant circuits of the same fluid to decrease the energy ingress in the low temperature environment are described. The goal is to achieve long lengths between cooling stations along the transmission line.

8.1. Introduction

In the sections above, means of minimizing the refrigerator loads and the temperature excursion of the superconductors were investigated. Means of decreasing the current-lead

cryogenic loads by about a factor of 2 were analyzed, as well as means of minimization of the temperature excursion in the superconductor. The innovation consisted of the use of intermediate cooling stations to intercept the thermal load from the room temperature environment, as well as the use of different coolant and/or coolant circuits to separately cooling the current leads and the superconductor. Although the use of two-stage cooling for low temperature operation (with an intermediate temperature around 80 K) has been proposed and explored in the past[18, 22], the contribution by Bromberg was to extend the principle to operation between room temperature and ~ 80K. The temperature of the intermediate stage that cools the current leads needs to be around about 160 or below in order to minimize the heat load to the superconductor substantially. Several fluids have been proposed in section 8.4 that could operate in the region of interest[25].

In addition to current leads, another source of heat to the cryogenic environment is through thermal radiation. The use of multiple stage cooling stations has been proposed for the minimization of the refrigerator electrical power requirement[28]. In that report it was shown that the use of an intermediate cooling stations can decrease the power requirement by a factor of two, while with the use of three thermal shields, the power can be decreased by a factor of 4. Although it is common to use intermediate cooling stations between room temperature and liquid helium environments, to our knowledge their use at elevated temperatures to minimize the thermal load at the ~ 75 K environment of HTS cables have not been suggested.

In this report, the topologies required to implement the use of using multiple cooling stages for minimization of the cryogenic load are analyzed. Also, means of facilitating long transmission lines are discussed.

8.2. Multiple Temperature Anchors

Figure 8.1 shows a schematic diagram of a cryostat where in each cryostat there are two cooling circuits, low temperature coolant and intermediate temperature coolant, either going in the same direction or in opposite directions. When in opposite direction, continuity of nitrogen flow is easily established and a single cryostat can close the loop, with a refrigerator at one end. The superconductor is in the cold circuit, with the warmer circuit cooling the intermediate cooling station. It is useful to provide thermal insulation or a vacuum gap to limit thermal conduction and convection from the intermediate temperature coolant to the low temperature coolant circuit. In Fig. 8.1 the return path is shown cooling only the intermediate cooling station, as would be the case for long distance transmission. For distribution systems, it would be possible to use the intermediate temperature coolant to also cool the current leads, in order to intercept the thermal energy at the higher temperature that would otherwise end up heating the superconductor coolant.
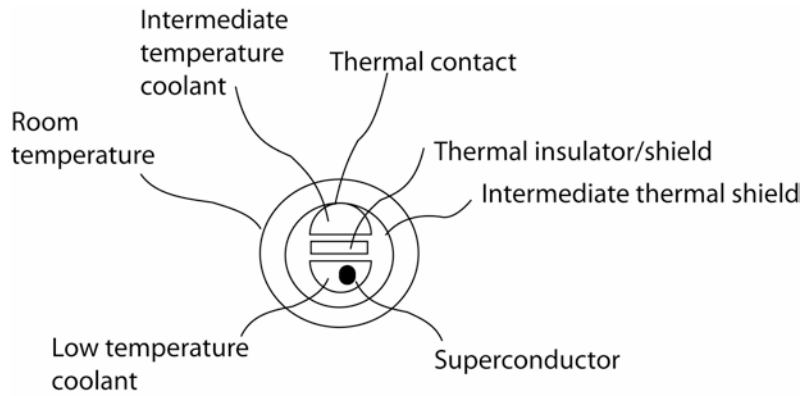
Fig. 8.1. Schematic diagram of a non-coaxial two-coolant system that separates the cooling of the thermal shield from that cooling the superconductor.

It is possible to taper the flow paths, in case that there is coolant transfer from the low temperature coolant to the intermediate temperature one, as for example when cooling a secondary current lead as discussed in the accompanying report[23]. Although the current leads would operate at slightly higher temperatures than the superconductor in this arrangement, heat ingression into the cold fluid path that cools the superconductor is decreased.

An alternative arrangement would have a coaxial arrangement of the different elements, as shown in Fig. 8.2. In this case, the thermal insulator or the vacuum gap is a concentric hollow cylinder. The intermediate temperature coolant is on the outside, while the low temperature coolant is in the central region.

The arrangement in Fig. 8.1 does not require that the temperature anchor be a single solid tube, as it could be a tube with an axial cut, but with overlapping lips in order to prevent radiation from streaming between the gap that would otherwise exist. The warm coolant is in a pipe, with the temperature anchor cooled by thermal conduction to this pipe. As depicted, the heating of the low temperature coolant, and thus the superconductor, would come from convection in the vacuum, conduction through support and from losses in the superconductor, if any. In the absence of losses in the superconductor, (as would be the case for DC systems), the heat ingress into the low temperature coolant path can be decreased by approximately two orders of magnitude.
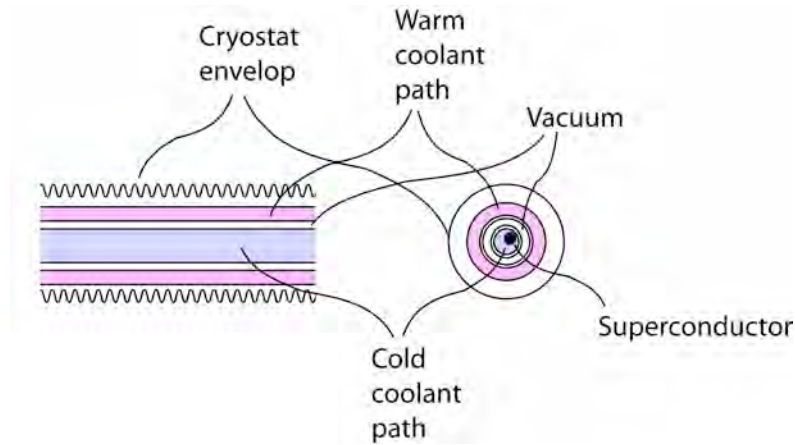
Fig. 8.2. Schematic diagram of a coaxial arrangement

The minimization of the heat ingression into the cold coolant path allows for the minimization of the low temperature coolant throughput or would allow for increased lengths of transmission line for a given throughput.

It is possible to use two different fluids for the cold loop and the warm loop. Miles described the optimal temperature of the intermediate cooling station (around 170K for a single stage)[28], while Bromberg [23]identified potential fluids that could be used.

8.3. Performance of Cooling Topologies for Transmission Systems

In this section, the performance of the several option discussed in Section II is assessed. It is not the goal of these calculations to fully optimize the system, as much more work needs to be done, including detailed investigation of the performance of the refrigerators. Instead, the goal is to provide insight into the potential of the different options for reducing the heat load.

The calculations have been performed for a long transmission line. The distributed cryostat losses dominate the thermal input in the case of the DC transmission. In this case it is also important to control the pressure drop along the line. It is also desirable to minimize the power requirements for the refrigerators.
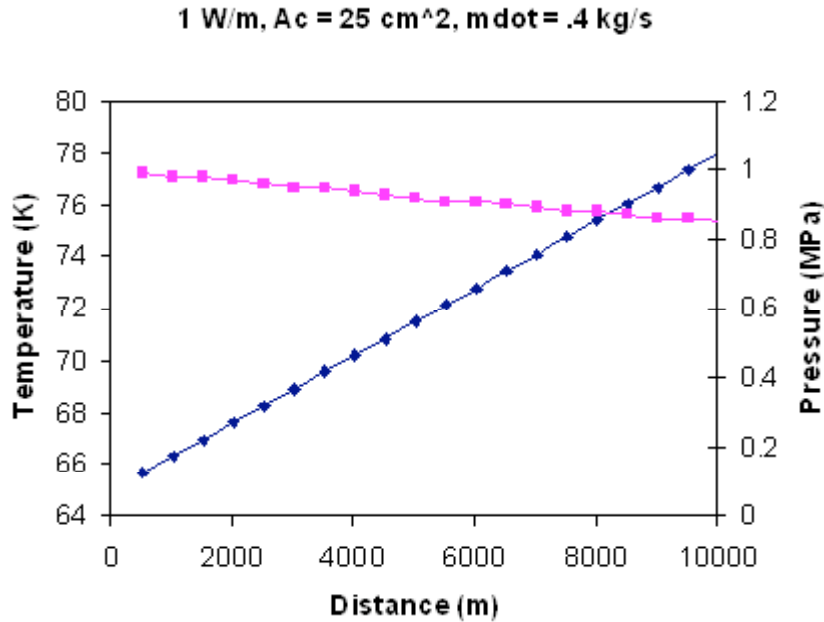
1 W/m, Ac = 25 cm^2, mdot = .4 kg/s

Fig. 8.3. Temperature and pressure along a 10 km transmission line. Cross sectional area of coolant is 25 cm^2 and the flow rate is 0.4 kg/s.

For the calculations, a compressible, steady state 1-1/2 D code has been used (CCAN), developed at MIT by Gierszewski[29]. CCAN calculates the temperature, pressure, power, and other engineering quantities along the length of an actively cooled electrical conductor. The code was developed to perform engineering analysis of internally cooled conductors, so it is particularly well suited for electrical power systems with distributed thermal loadings. The code assumes single-phase flow and neglects axial conductions relative to heat transfer to the coolant. It is assumed that the refrigerators operate with 20% of Carnot efficiency, an aggressive goal corresponding to the middle term expectations from the Navigant study [11].

It is assumed that the inlet pressure is 10 bar, and that there are no large elevations/depressions in the line, so that the pressure is determined mainly by hydraulic losses from the flow. Elevation of 10's of meters would not change the results much, but much larger changes in elevation would require more detailed calculations. This is particularly important towards the end of the transmission line, where two-phase flow may be generated with decreased pressure due to an increase in elevation.

Figure 8.3 shows the results of the calculations for a conventional [3, 26, 27] transmission line, where a single coolant cools the superconductor and the inner cryostat. It has been assumed that the length of the section to be cooled with a single refrigerator is 10 km. This number is arbitrary, but it is felt that much lower distances for each independently cooled section would not be an attractive solution for transmission. In order to be able to remove the heat over 10 km (~ 10 kW) with a small ΔT, the mass flow rate needs to be ~ 0.4 kg/s. In order to prevent an excessive pressure drop, the cross sectional area of the coolant is ~ 25 cm^2. Although the temperature rise of the coolant is

not excessive (around 13 K), it has substantial impact on the superconductor performance. For fields perpendicular to the tape, the critical current density of second generation HTS drops by about at factor of 2.5-3 in the presence of a modest field (0.4 T) when the temperature is raised form 65 K to 77 K. The pressure drop has been limited to about 0.2 MPa (2 bar).

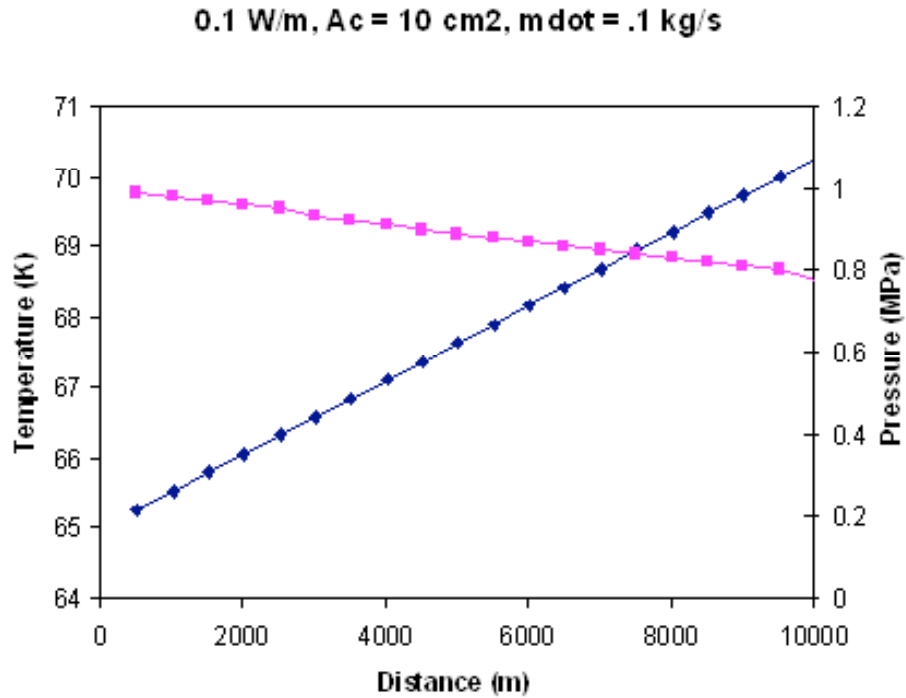**0.1 W/m, Ac = 10 cm2, m dot = .1 kg/s**

Fig. 8.4. Temperature and pressure along the line for the low temperature coolant circuit, when there is an intermediate cooling station at 160 K.

Figure 8.4 shows the results of the simulation when there is an intermediate cooling station at 160 K. In this case, the thermal energy input to the low temperature coolant is reduced by more than an order of magnitude (reduced by a factor of $\sim (160/300)^4$), resulting in ~ 0.1 W/m. In this case, it is possible to cool long lengths of the transmission line with relatively small temperature rise in the cold stream, ~5 K, with substantially smaller cross sectional area (10 cm^2). The flow rate of the coolant is about 4 times lower in the cold stream, resulting in comparable pressure drop.
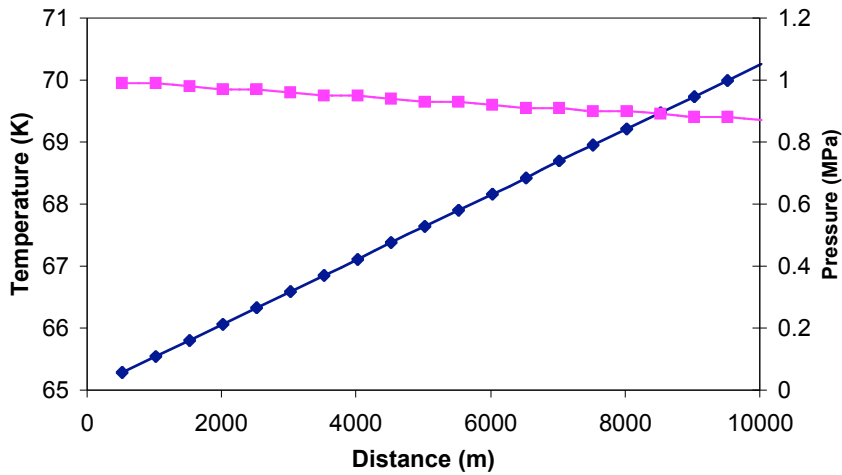
.01 W/m, Ac = 4 cm^2. mdot = .01 kg/s

Fig. 8.5. Temperature and pressure along the low temperature coolant circuit for the case of an intermediate cooling station at around 90K.

Figures 8.5 and 8.6 cover the case when there is a intermediate cooling station is at 90 K, which further decreases the radiated power to the environment of the low temperature coolant. In this case, it is assumed that radiated power to this environment is 0.01 W/m (~ $(90/300)^4$). The 90 K environment, on the other hand, is removing 1 W/m (the full thermal load from the room temperature environment). Figure 8.5 shows the temperature and the pressure on the low temperature coolant circuit, while Fig. 8.6 shows those parameters for the intermediate temperature circuit.

For the low temperature coolant circuit, the flow rate requirements, as well as the cross sectional area for coolant, have decreased substantially for the low temperature coolant circuit, to 0.01 kg/s and 4 cm^2, respectively. The pressure drop is a modest 1 bar, over 10 km. The temperature rise has been kept constant to about 5 K. By comparison, the high temperature coolant circuit, which needs to remove 1 W/m, has a temperature rise of 20 K, a cross sectional area of 19 cm2, and a pressure drop of about 2 bar.
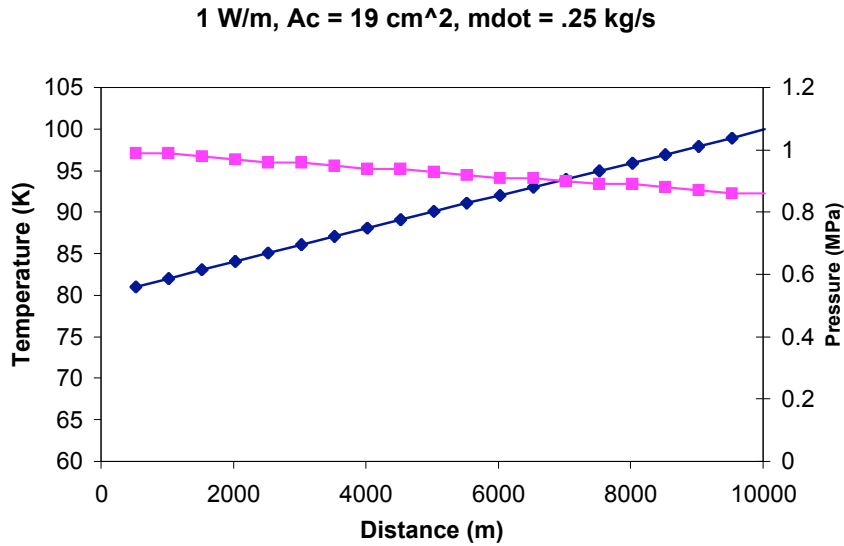
Fig. 8.6 Temperature and pressure along the intermediate temperature coolant circuit.

It is interesting to note that the total cross sectional area did not change much (24 cm^2 in Fig. 8.4 and 8.5, vs. 25 cm^2 in Fig. 8.5. The reason for this is that the total heat that needs to be removed is the same (1 W/m), and the temperature rise is comparable (13 K in Fig. 8.3, 20 K in Fig. 8.6). The total required refrigeration power is reduced, however, because of the heat appears mostly in the high temperature stream, resulting in a high thermodynamic efficiency. In order to be able to decrease the cross sectional area, other fluids can be used. As shown in Table 7.4 [23], methane or argon are attractive candidates, as they could remove about twice as much heat for the same pressure drop. The intermediate temperature circuit would operate at higher temperatures.

Table 8.1 shows the comparison between two of the cases analyzed in this section. The baseline case, which uses the same coolant for cooling the superconductor as well as the cryostat, with no intermediate cooling station, and a case with a intermediate temperature station operating at 80-100 K (*i.e.*, using liquid nitrogen). The main parameters of the simulation are presented, including energy ingress (Q), mass flow rate (mdot), inlet, and outlet temperature of the respective topology (Tinlet and Toutlet), pressure drop (Δp) and cross sectional area (Ac). Also shown is the refrigerator power (assuming 20% Carnot). In the baseline case, the refrigerator power (with an outlet at 65 K), is about 160 kW. In the case with the intermediate cooling station, the total refrigerator power is about 120kW. The refrigerator with an outlet temperature of 80 K consumes about all of the power, with less than 2% for the low outlet temperature (65 K) refrigerator.

It should be noted that the reduction in the refrigerator power of about 1.4 in Table 8.1 is substantially lower than the reduction predicted by Miles[28]. The reason is that the purpose of the minimization in this section is to decrease the thermal ingress to the low temperature circuit, rather than minimizing the refrigerator power. The refrigerator power is minimized by operating the intermediate circuit around 160 K, with a

substantially lower outlet temperature for the cold stream than the single stream in the baseline case.

Table 8.1
Summary of results comparing base case to a case with one intermediate cooling station at a

		Base case	One intermediate stage	
			High T	Low T
Q	W/m	1	1	0.01
mdot	kg/s	0.4	0.25	0.01
Tinlet	K	65	80	65
Toutlet	K	78	100	70
Δp	MPa	0.18	0.18	0.18
Ac	cm^2	25	19	4
Refrigerator power	kW	162	118	1.8

temperature around 90 K

8.4. Calculations of Maximum Length Cooled With Single Coolant

The above model can be used to determine the limits to the cooling lengths, for fixed conditions. In this section, the maximum cooling length is calculated for a thermal load of 1 W/m, for constant elevation (so that there are no excursions in pressure due to gravity), and for two different cross sections of the coolant flow.
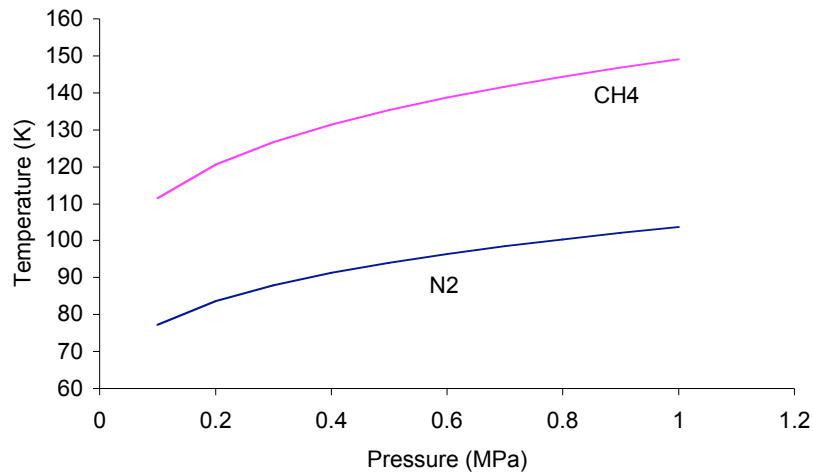

Fig. 8.7. Boiling temperatures of nitrogen and methane as a function of pressure.

There are multiple limitations, but in this section the one due to subcooled boiling is investigated, with only single-phase flow permitted. Boiling occurs at a temperature that increases with pressure. Figure 8.7 shows the boiling temperature of nitrogen and methane for different pressures, produced from the NIST database [30]. Methane is an attractive alternative coolant for the intermediate cooling station, as discussed in section 7.4 [23]. Although phase change offers large changes in enthalpy (200 kJ/liter for nitrogen), gas generation within the line results in unpredictable flow, and the possibility of vapor lock, although Ashworth has proposed the use of two channels with gas on one channel and liquid on the other [31].
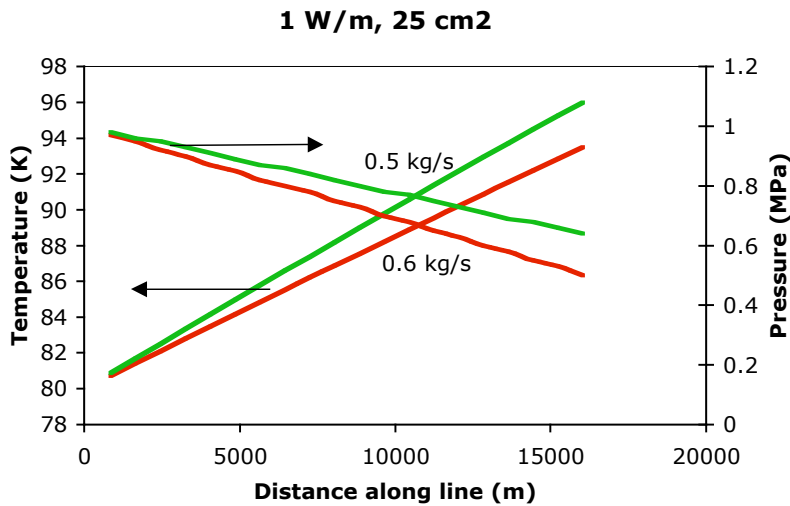
1 W/m, 25 cm2

Fig. 8.8.   *Temperature and pressure for 1 W/m and of 25 cm^2 coolant cross sectional area without subcooled boiling.*
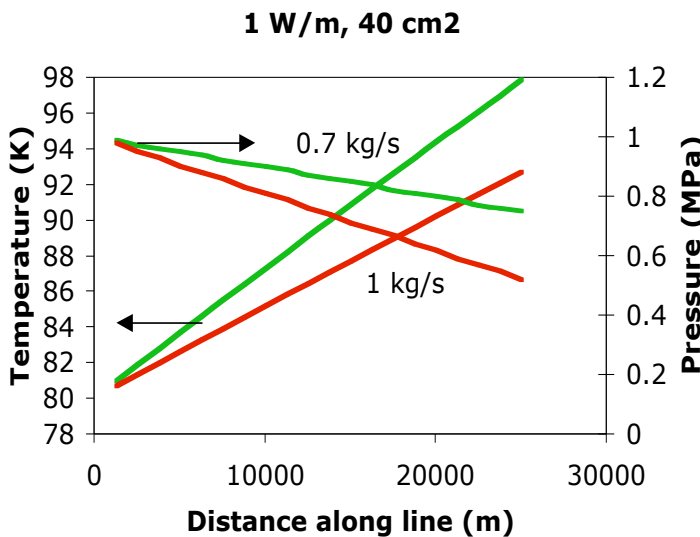
1 W/m, 40 cm2

Fig. 8.9. *Same as Fig. 8.7, but for a cross sectional area of the coolant of 40 cm^2.*

60

On the one hand, faster flows result in lower temperatures at the exit, but on the other hand, faster flows result in lower pressure at the outlet due to increased pressure drop at the higher flow rates. The goal of this section is to explore this tradeoff. Larger cooling cross sections for the intermediate temperature stage allow increased flow rates, or lower pressure drop for a given flow rate. In this section, the two arbitrarily chosen cross sections are 25 cm^2 and 40 cm^2.

The temperature and pressure along the transmission line are shown in Fig. 8.8 for the case of 25 cm^2 and in Fig. 8.9 for the case of 40 cm^2. In both cases, the results are limited by avoidance of subcooled boiling. In Figs. 8.8 and 8.9, there is little difference between the high flow rates and the lower flow rates, as the lower temperature in the case of higher flow rates results in lower pressures (and thus lower subcooled boiling temperature) than the case with lower flow rate. There is little difference in the length of the transmission line that can be cooled without recool for the different flow rates chosen in Figs. 8.8 and 8.9.

Table 8.2 summarizes the results for the limited cases investigated in this section. The main conclusion is that subcooled boiling represents a limitation that, for a given cross section, seems to limit the cooling length to about 15-25 km, for the case of 1 W/m, 10 bar inlet pressure, and little changes in elevation. The row marked Power (W) in Table 8.2 refers to the electrical power at room temperature, assuming 20% Carnot efficient refrigerators, The pumping power is a very small fraction of the total electrical requirements.

Table 8.2.
Comparison of high and low flow rates, for two different coolant cross sections

	25 cm2		40 cm2	
	High flow rate	Low flow rate	High flow rate	Low flow rate
Length (m)	16000	16000	25000	25000
Flow rate (kg/s)	0.6	0.5	1	0.7
Inlet temperature (K)	80	80	80	80
Outlet temperature (K)	93.5	96	92.7	97.8
Inlet pressure (Mpa)	1	1	1	1
Outlet pressure (Mpa)	0.5	0.64	0.52	0.75
Power (W)	204	197	321	302

8.5. Summary

Different cooling circuit topologies for long-distance distribution systems have been evaluated in this report. Means of eliminating substantial temperature rise of the superconductor have been found, through the use of multiple coolants or multiple coolant circuits (operating at different temperatures). Long transmission lines can be cooled in

this manner, using either liquid nitrogen both circuits, or liquid nitrogen for the low temperature circuit and a different fluid for the intermediate temperature circuit.

The purpose of this report, and the accompanying one, is not to optimize the system. To do so requires substantially more work, better understanding of refrigerator performance as a function of capacity and temperatures and inclusion of the small but finite thermal conduction and convection thermal ingress, especially to the low temperature circuit. However, the work does show the potential of the method for addressing key issues on implementation of HTS cables for transmission and distribution.
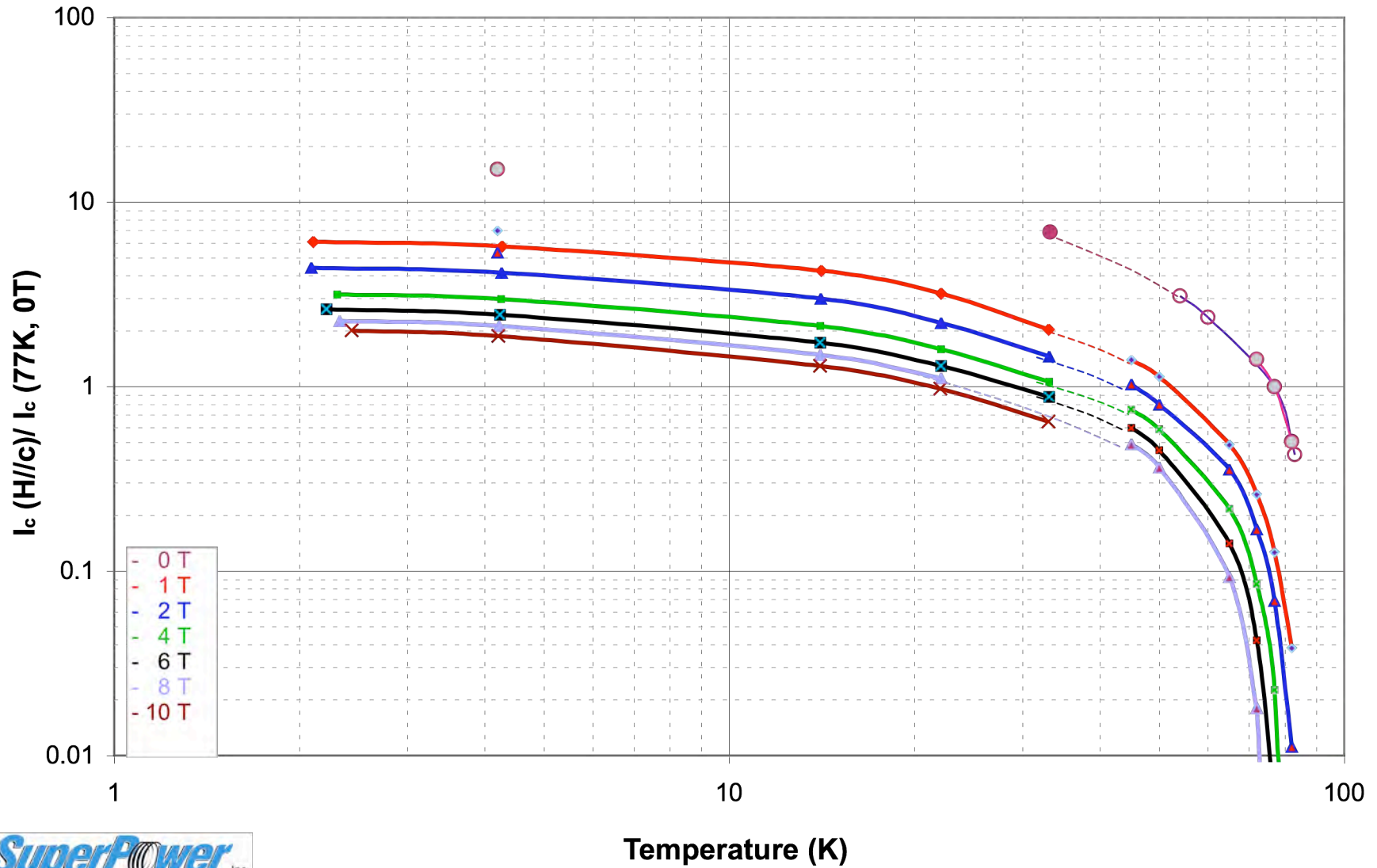
It has been determined that it is possible to decrease the refrigeration power by about a factor of 2 for both cryostat loads and the current leads, while allowing for low temperature rise in the low temperature circuit, facilitating long sections between recool for transmission lines.
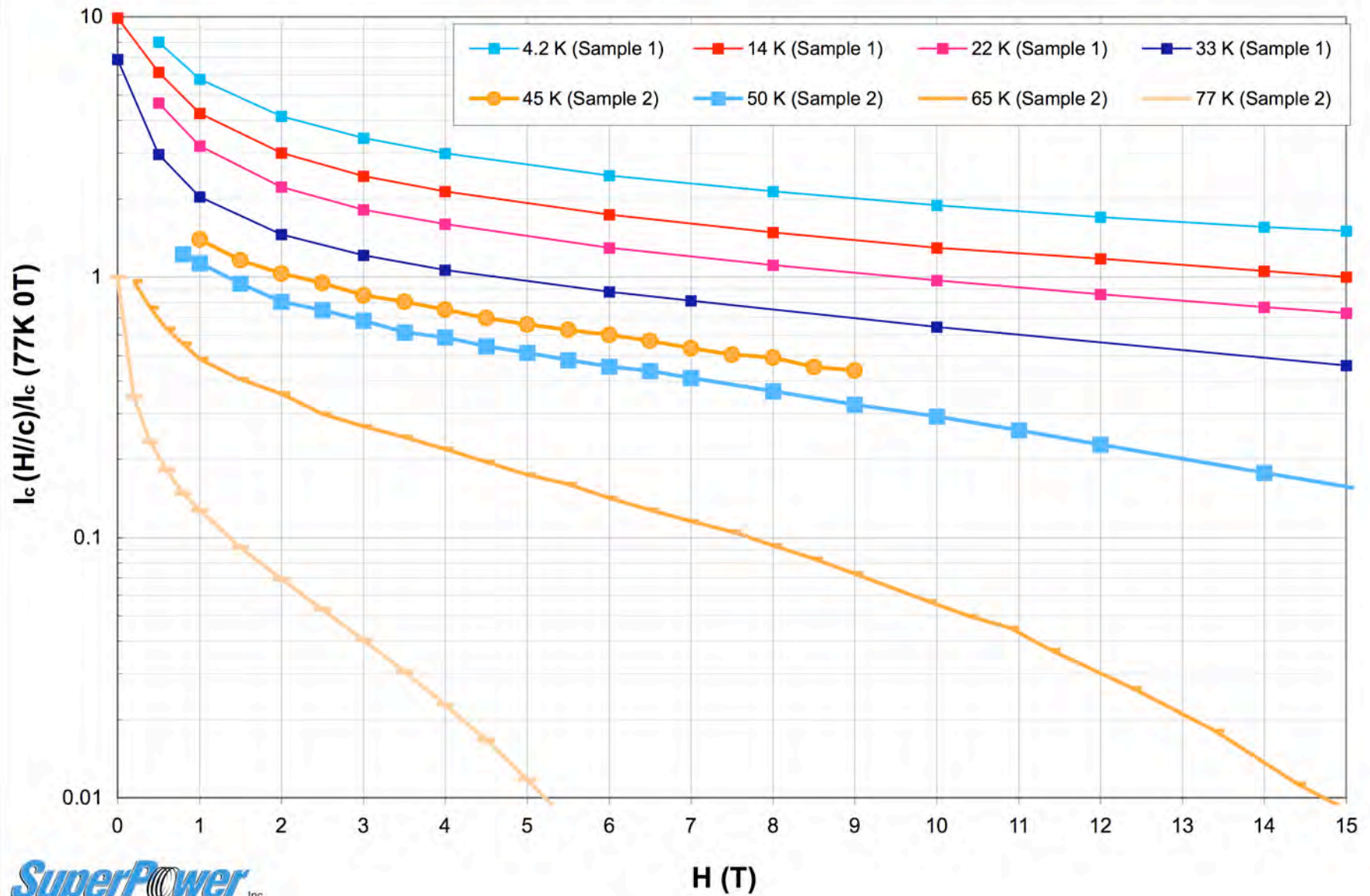
9. References

1. Dietz, A.J., et al., *Resistance of Demountable Mechanical Lap Joints for a High Temperature Superconducting Cable Connector.* IEEE Transactions on Applied Superconductivity, June 2008. **18**(2): p. 1171-1174.
2. Koomey, J., *Estimating total power consumption by servers in the U.S. and the world*. 2007, Lawrence Berkeley National Laboratory: Oakland, CA, Avaliable from http://enterprise.amd.com/us-en/AMD-Business/Technology-Home/Power-Management.aspx.
3. Maguire, J.F., et al., *Development And Demonstration Of A HTS Power Cable To Operate In The Long Island Power Authority Transmission Grid.* IEEE Transactions on Applied Superconductivity, 2007. **17**: p. 2034-7.
4. Haught, D. and e. al., *Overview of the U.S. Department of Energy (DOE) High-Temperature Superconductivity Program for Large-Scale Applications.* International J. Applied Ceramic Tech, July 2007. **4**: p. 197-202.
5. Demko, J.A., et al., *Triaxial HTS Cable for the AEP Bixby Project.* IEEE Transactions on Applied Superconductivity. **17**: p. 2047-2050.
6. *DOE Superconductivity Peer Review 2008*. Available from: http://www.energetics.com/supercon08/.
7. Yamaguchi, T., et al., *Experimental and numerical characteristics of peltier current lead for direct current mode.* IEEE Transactions on Applied Superconductivity, 2004. **14**: p. 1719-1722.
8. Pratt, A., P. Kumar, and T.V. Aldridge, *Evaluation of 400V DC Distribution in Telco and Data Centers to Improve Energy Efficiency*, in *29th International Telecommunications Energy Conference, INTELEC 2007*. 2007, IEEE: Rome, Italy. p. 32-39.
9. *DC Power For Data Centers of the Future*. Available from: http://hightech.lbl.gov/dc-powering.
10. Ton, M., B. Fortenbery, and W. Tschudi, *DC Power for Improved Data Center Efficiency*. 2008, Lawrence Berkeley National Laboratory: Berkeley, CA. p. 3-4.
11. NavigantConsulting. *High Temperature Superconductivity Market Readiness Review*. 2006; Available from: http://www.energetics.com/meetings/supercon06/pdfs/Plenary/07_Navigant_HTS_Market_Readiness_Study.pdf.
12. Iwasa, Y. Private communication to L. Bromberg: Cambridge, MA.
13. Dewar, L., *Collected papers for Sir James Dewar*. 1927, Cambridge, England: Cambridge University Press.
14. Weisend II, J.G., et al, *Handbook of Cryogenic Engineering*. 1998, Philadelphia, PA: Taylor and Francis.
15. Strobridge, T.R., *Cryogenic Refrigerators, An Updated Survey, NBS Tech Note 655*. 1974, US Department of Commerce.

16. Weber, C.S., et al., *Testing and Demonstration Results of the 350 m Long HTS Cable System Installed in Albany, NY.* IEEE Transactions on Applied Superconductivity, 2007. **17**: p. 2038-42.

17. Sohn, S.H., et al., *The Results of Installation and Preliminary Test of 22.9 kV, 50 MVA, 100 m Class HTS Power Cable System at KEPCO.* IEEE Transactions on Applied Superconductivity. **17**: p. 2043-2046.

18. McFee, R., *Optimum Input Leads for Cryogenic Apparatus.* Rev Scientific Instr., 1959. **30**.

19. Rasmussen, C.N. and e. al., *Optimization Of Termination For A High-Temperature Superconducting Cable With Room Temperature Dielectric Design.* IEEE Trans. Appl. Supercond., 1999. **9**: p. 45-49.

20. *Materials Properties Database.* Cryogenic Technologies Group of NIST; Available from: http://cryogenics.nist.gov/MPropsMAY/material%20properties.htm.

21. NIST, *Cryogenic Properties of Materials.* 1973.

22. Iwasa, Y., *Case Studies of Superconducting Magnets.* 1994, New York: Plenum Press.

23. Bromberg, L., P. Michael, and J. Minervini, *Current Lead Optimization for Cryogenic Operation at Intermediate Temperatures.* 2008, MIT Plasma Science and Fusion Center Report, PSFC-JA-08-09.

24. Furuse, M., S., et al., *Feasibility Study of Low-Voltage DC Superconducting Distribution System,.* IEEE Trans Applied Superconductivity, 2005. **15**: p. 1759.

25. Bromberg, L. and J. Minervini, *Cooling Topologies for Superconducting Power Systems: I. Short-Distance Electric Distribution.* 2008, MIT Plasma Science and Fusion Center Report: PSFC/JA-08-33.

26. Lee, R.C., A. Dada, and S.M. Ringo, *Cryogenic Refrigeration System for HTS Cables.* IEEE Trans. Appl. Superconductivity, 2005. **15**: p. 1798.

27. Rostila, L., et al., *Design of a 30 m long 1 kA 10 kV YBCO cable.* Supercond. Sci. Technol., 2006. **19**: p. 418-422.

28. Miles, C., et al., *Cryostat Optimization Through Multiple Stage Thermal Shields.* 2008, MIT Plasma Science and Fusion Center Report: PSFC/JA-08-19.

29. Gierszewski, P.J., A.S. Wan, and T.F. Yang, *CCAN and TCAN – 1 – 1/2 D Compressible Flow and Time Dependent Codes for Conductor Analysis.* 1983, MIT Plasma Science and Fusion Center Report: PSFC/RR-83-01

30. Lemmon, E.W., M.L. Huber, and M.O. McLinden, *REFPROP, Reference Fluid Thermodynamic and Transport Properties.* 2007, NIST Standard Reference Database 23, Version 8

31. Ashworth, S., T. Jankowwsli, and D. Gardner. *Advanced Cable Research.* High Temperature Superconductivity Program Peer Review 2008; Available from: http://www.energetics.com/supercon08/agenda.html.

I_c/I_c (77K, 0T) vs. Temperature in perpendicular field

Temperature (K)

Vertical axis: I_c (H//c)/ I_c (77K, 0T)

Legend:
- 0 T
- 1 T
- 2 T
- 4 T
- 6 T
- 8 T
- 10 T

SuperPower Inc.

I_c/I_c (77K, 0T) vs. Field (perpendicular)

10. Appendix I. High Temperature Superconductor Properties